EFFECT OF HEAT TREATMENT PRODEDURES ON MICROSTRUCTURE AND MECHANICAL PROPERTIES OF NODULAR IRON

A THESIS SUBMITTED
IN PARTIAL FULFILMENT OF THE REQUIREMENT FOR THE DEGREE OF

Master of Technology

In

Metallurgical and Materials Engineering

By

Anita Bisht

Department of Metallurgical and Material Engg.
Rourkela, India

June 2009

EFFECT OF HEAT TREATMENT PRODEDURES ON MICROSTRUCTURE AND MECHANICAL PROPERTIES OF NODULAR IRON

A Thesis Submitted to
National Institute of Technology, Rourkela
(Deemed University)

In partial fulfilment of the requirement for the degree of
Master of Technology

In
Metallurgical and Materials Engineering

By

Anita Bisht
(Roll No. 207mm110)

Under the guidance and supervision of

Dr. Sudipta Sen
&
Dr. Subash Chandra Mishra

Metallurgical and Materials Engineering

CERTIFICATE

This is to certify that the work in the thesis report entitled as, **"Effect Of Heat-Treatment Procedures On Microstructures and Mechanical Properties Of Nodular Iron",** which is being submitted by Km. Anita Bisht of Master Of Technology (Roll No. 207mm110), from National Institute Of Technology, Rourkela has been carried out under my guidance and supervision for the partial fulfillment of the requirement for the degree of Master of Technology in Metallurgical and Materials Engineering and it is a bonafide record of work.

Dr. S.C.Mishra (Co-Guide),
Professor,
Deptt.of Matallurgical and Materials Engg.
NIT, Rourkela.

Dr.S.Sen (Guide),
Asst. Professor,
Deptt of Metallurgical and Materials Engg.
NIT, Rourkela.

ACKNOWLEDGEMENT

I avail this opportunity to extend my hearty indebtedness to my guide **Dr**. **Sudipta Sen** for his invaluable guidance, untiring efforts and meticulous attention at all stages during my course of work. I would also like to convey my deep regards to my co-guide **Dr.S.C.Mishra** for his patience, constant motivation and regular monitoring of the work and inputs, for which this work has come to fruition.

I express my gratitude to **Prof. B B Verma, Head of the Department** for providing me the necessary facilities in the department.

I am also thankful to **Mrs Tabasum Ara Begum, Sri Hemram, Sri Udayanath Sahu, Sri Rajesh Pattnaik, and Sri Samir Pradhan,** Metallurgical & Materials Engineering, Technical assistants, for their co-operation in experimental work.

Anita Bisht

Abstract

In their bid to produce cast iron latter than Malleable Iron, the scientist discovered the ductile iron or S.G. Iron (spherodial Graphite iron) way back in 1948.The use of this type of cast iron as an engineering material has been increasing day by day ever since its discovery. It is now replacing steel in many important engineering applications. The production of S.G Iron increased to a large extent during last two decades.

The excellent combination of mechanical properties obtained in S.G. iron can further be informed by the heat treatment. The most recent development in this regard is the production of Austempered Ductile Iron (ADI).It provides an excellent combination of high tensile strength, wear resistance along with good corrosion resistance and quite significant amount of ductility.

Due to these factors, S.G. or ductile iron are austempered when a very favourable combination of various properties is required. But this type of treatment is bit tricky,since it require controlled heating and isothermal holding of the material. So it is necessary to find some attractive methods for property development in S.G. iron.

In the present work conventional heat treatment proceeds like annealing, normalizing and tempering of the material has been performed. The mechanical properties obtain by various technique have been compared to one another.In this work two different grades of S.G. Iron (one with copper and another without copper) have been used. The effect of the alloying element (i.e. copper) has also been studied.

CONTENTS

Chapter 1

Chapter 2

Chapter 3

LIST OF FIGURES

LIST OF TABLES

CHAPTER 1

Introduction

CHAPTER1

1. Introduction:

Ductile Iron also referred to as **"Nodular Iron"** or Spheriodial graphite iron was patented in 1948.After a decade of intensive development work in the 1950's, ductile iron had a phenomenal increase in the use as an engineering material during the 1960's, and the rapid increase in commercial application continues today.[1]

An unusual combination of properties is obtained in ductile iron because the graphite occurs as spheroids rather than as graphite flakes as in grey iron. This mode of solidification is obtained by adding a very small, but specific amount of Mg & Ce or both to molten iron of proper composition. The base iron is severely restricted in the allowable contents of certain minor elements that can interfere with graphite spheroid formation. The added Mg reacts with S or O in the melt or molten iron and the way the graphite is formed. Control procedures have been developed to make the processing of ductile iron dependable.[1]

The high C & Si content of ductile iron provide the casting process advantageous, but the graphite nodules have only the nominal influence on the mechanical properties of the melt. Ductile iron, like malleable iron, exhibits a linear stress- strain ratio, a considerable range of yield strengths and as it's name implies, ductility. Castings are made in a wide range of sizes with sections which are very thin or very thick. [2]

The different grades are produced by controlling the matrix structure around the graphite either the as cast or by subsequent heat treatment. Only minor compositional differences exist among the regular grades, and these adjustments are made to promote the desired matrix microstructures. Alloy addition may be made to abet in controlling the matrix structure as-cast to provide response to heat treatment. Special analysis ductile iron and high alloy ductile irons provide unusual properties for special application. [1, 3]

1.1 Birth Of Ductile Iron

In spite of the progress achieved during the first half of 20th century in the development of Gray and malleable Irons, foundry men continued to search for the ideal cast iron – an as cast "gray iron" with mechanical properties equal to superior to Mellable Iron. J.W. Bolten speaking at the 1943 convention of the American Foundrymen's Society (AFS), made the following statement. "Your indulengence is requested to permit the posing of one question. Will real control of graphite shape be realized gray iron? Visualization a material, processing (as cast) graphite flakes or grouping resembling those of mellable iron instead of elongated flakes."

A few weeks later, in the International Nickel Company Research Laboratory, Keith Dwight Millis made a ladle addition of magnesium (as a copper-magnesium alloy) to cast iron and justified Bolton's optimism- the solidified castings contained no flakes, but nerely perfect spheres of graphite. **Ductile iron was born!** At the time of Morrogh's presentation, the International Nickel Company revealed their development, starting with Millis' discovery in 1943, of magnesium as a graphite spherodizer. On October 25, 1949, patent 2,486,760 was granted to the International Nickel Company, assigned to Kieth D. Millis, Albert P. Gegnebin and Norman B. Pilling. This was the official birth of Ductile Iron, the beginning of 40 years of continual growth worldwide, inspite of recessions and changes in materials technology and usage. [1]

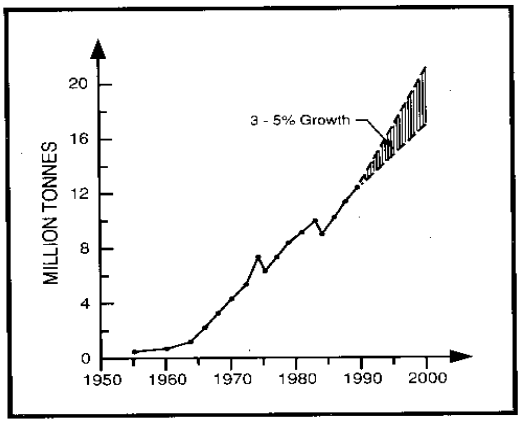

Fig 1.1 worldwide growth of ductile iron

1.2Various grade of S.G. irons accepted as per international norms are given below:

International standard ISO 1083: 1987[4]

Grade	Tensile Strength (N/mm^2)	0.2 % Proof Strength (N/mm^2)	Elongation (%)
900-2	900	600	2
800-2	800	480	2
700-2	700	420	2
600-3	600	370	3
500-7	500	320	7
450-10	450	310	10
400-15	400	250	15
400-18	400	250	18
400-18L	400	250	18
350-22	350	220	22
350-22L	350	220	22

1.3 Chemical Composition:

Chemically this material is same as gray iron and is Fe-C-Si alloy. It led to the development of cast iron technology since 1948. As the name suggests, it was developed to overcome the brittle nature of gray and white irons. It is quite ductile in as-cast form

and negates the need for long heat treatments such as those required to produce malleable iron.[5]

1.4Microstructure:

Fig 1.2 Microstructure of gray and ductile iron

Engineering applications of cast iron have been traditionally based upon gray (Flake graphite) irons providing a range of tensile strengths between about 150 N/mm^2 and 400 N/mm^2 with recommended design stresses in tensile applications of 0.25 x tensile strength. Despite their limited strength gray irons provided very useful l combinations of properties, which have ensured there wide continuing use. In fact gray irons still account for nearly 70 % of all iron castings produced. In contrast ductile irons have tensile strengths ranging from 350 to 1500 N/mm^2 with good elongation and high toughness. They now account for about 25 % of iron casting production serving in safety critical applications where they have replaced steel casting, forging and fabrications with technical and cost advantage.[5]

The main difference between ductile iron and gray iron is the morphology of graphite particles as shown in figure 1.2 which take on a nodular or almost spherical form after suitable treatments are made to the melt. The major micro structural constituents of ductile iron are: the chemical and morphological forms taken by carbon, and the continuous metal matrix in which the carbon and/or carbides are dispersed. [5]

The following important micro structural components are found in ductile iron.

1.4.1Graphite

This is the stable form of pure carbon in cast iron. Its important physical properties are low density, low hardness and high thermal conductivity and lubricity. Graphite shape, which can range from flake to spherical, plays a significant role in determining the mechanical properties of cast irons. Figures 1.3 (a) and (b) show that graphite flakes act like cracks in the iron matrix, while graphite spheroids act like "crack arresters", giving the respective irons dramatically different mechanical properties.[6]

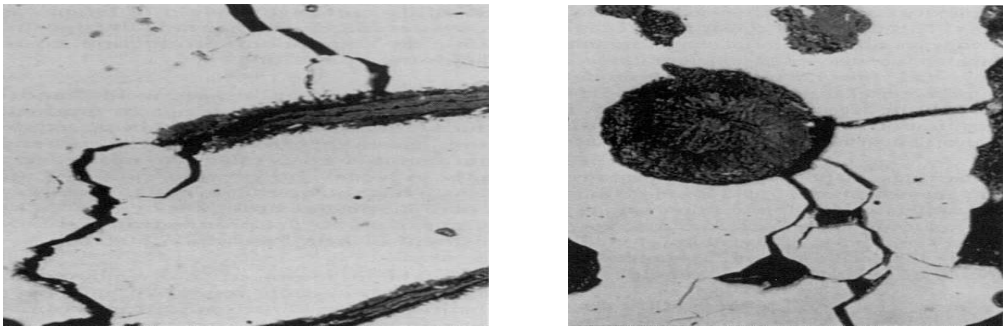

(a) (b)

Fig 1.3: graphite nodules as a crack arrester.

1.4.2 Carbide:

Carbide, or cementite, is an extremely hard, brittle compound of carbon with either iron or strong carbide forming elements, such as chromium, vanadium or molybdenum. Massive carbides increase the wear resistance of cast iron, but make it brittle and very difficult to machine. Dispersed carbides in either lamellar or spherical forms play in important role in providing strength and wear resistance in as-cast pearlitic and heat-treated irons.[6]

1.4.3 Ferrite:

This is the purest iron phase in a cast iron. In conventional Ductile Iron ferrite produces lower strength and hardness, but high ductility and toughness. In

Austempered Ductile Iron (ADI), extremely fine-grained accicular ferrite provides an exceptional combination of high strength with good ductility and toughness.[6]

1.4.4Bainite:

Bainite is a mixture of ferrite and carbide, which is produced by alloying or heat treatment.[6]

1.4.5 Pearlite:

Pearlite, produced by a eutectoid reaction, is an intimate mixture of lamellar cementite in a matrix of ferrite. A common constituent of cast irons; pearlite provides a combination of higher strength and with a corresponding reduction in ductility which meets the requirements of many engineering applications.[6]

1.4.6Martensite:

Martensite is a supersaturated solid solution of carbon in iron produced by rapid cooling. In the untempered condition it is very hard and brittle. Martensite is normally "tempered" - heat treated to reduce its carbon by the precipitation of carbides - to provide a controlled combination of high strength and wear resistance.[6]

1.4.7Austenite:

Normally, a high temperature phase consisting of carbon dissolved in iron, it can exist at room temperature in austenitic and austempered cast irons. In austenitic irons, austenite is stabilized by nickel in the range 18-36%. In austempered irons, austenite is produced by a combination of rapid cooling which suppresses the formation of pearlite and the supersaturation of carbon during austempering, which depresses the start of the austenite-to-martensite transformation far below room temperature. In austenitic irons, the austenite matrix provides ductility and toughness at all temperatures, corrosion resistance and good high temperature proper-ties, especially under thermal cycling conditions. In austempered Ductile Iron stabilized austenite, in volume fractions up to 40% in lower strength grades, improves toughness and ductility and response to surface treatments such as fillet rolling.[6]

1.5Family of Ductile Irons:

With a high percentage of graphite nodules present in the structure, mechanical properties are determined by the Ductile Iron matrix. The importance of matrix in controlling mechanical properties is emphasized by the use of matrix names to designate the following types of Ductile Iron.

1.5.1Austenitic Ductile Iron:

Alloyed to produce an austenitic matrix, this Ductile Iron offers good corrosion and oxidation resistance, good magnetic properties, and good strength and dimensional stability at elevated temperatures.

1.5.2 Ferritic Ductile Iron:

Graphite spheroids in a matrix of ferrite provide an iron with good ductility and resistance and with a tensile and yield strength equivalent to a low carbon steel. Ferritic Ductile Iron can be produced "as-cast" but may be given an annealing heat treatment to assure maximum ductility and low temperature toughness

1.5.3. Ferritic Pearlitic Ductile Iron:

These are the most common grade of Ductile Iron and are normally produced in the "as cast" condition. The graphite spheroids are in a matrix containing both ferrite and pearlite. Properties are intermediate between ferritic and pearlitic grades, with good machinability and low production costs.

1.5.4Pearlitic Ductile Iron:

Graphite spheroids in a matrix of pearlite result in an iron with high strength, good wear resistance, and moderate ductility and impact resistance. Machinability is also superior to steels of comparable physical properties. The preceding three types of Ductile Iron are the most common and are usually used in the as-cast condition, but Ductile Iron can be also be alloyed and/or heat treated to provide the following grades for a wide variety of additional applications.[6]

1.5.5Martensitic Ductile Iron:

Using sufficient alloy additions to prevent pearlite formation, and a quench-and-temper heat treatment produces this type of Ductile Iron. The resultant tempered martensite matrix develops very high strength and wear resistance but with lower levels of ductility and toughness.

1.5.6Bainitic Ductile Iron:

This grade can be obtained through alloying and/or by heat treatment to produce a hard, wear resistant material.[6]

1.5.7Austempered Ductile Iron (ADI):

ADI, the most recent addition to the Ductile Iron family, is a sub-group of Ductile Irons produced by giving conventional Ductile Iron a special austempering heat treatment. Nearly twice as strong as pearlitic Ductile Iron, ADI still retains high elongation and toughness. This combination provides a material with superior wear resistance and fatigue strength.[6]

1.6 Production of Ductile Iron:

Ductile iron, also known as Spheroidal Graphite (S.G.) iron or nodular iron, is made by treating liquid iron of suitable composition with magnesium before casting. This promotes the precipitation of graphite in the form of discrete nodules instead of interconnected flakes. The nodular iron so formed has high ductility, allowing castings to be used in critical applications such as:

Crankshafts, steering knuckles, differential carriers, brake callipers, hubs, Brackets, valves, water pipes, pipe fittings and many others.

Ductile iron production now accounts for about 40% of all iron castings and is still growing. While a number of elements, such as cerium, calcium and lithium are known to develop nodular graphite structures in cast iron; magnesium treatment is always used in practice. The base iron is typically:

%C	%Si	%Mn	%S	%P
3.7	2.5	0.3	0.01	0.01

having high carbon equivalent value (CEV) and very low sulphur. Sufficient magnesium is added to the liquid iron to give a residual magnesium content of about 0.04%, the iron is inoculated and cast. The graphite then precipitates in the form of spheroids. It is not easy to add magnesium to liquid iron. Magnesium boils at a low temperature (1090°C), so there is a violent reaction due to the high vapor pressure of Mg at the treatment temperature causing violent agitation of the liquid iron and considerable loss of Mg in vapor form. This gives rise to the familiar brilliant 'magnesium flare' during treatment accompanied by clouds of white magnesium oxide fume. During Mg treatment, oxides and sulphides are formed in the iron, resulting in dross formation on the metal surface, this dross must be removed as completely before casting. It is important to remember that the residual magnesium in the liquid iron after treatment oxidizes continuously at the metal surface, causing loss of magnesium, which affects the graphite spheroids, moreover the dross formed may result in harmful inclusions.

Several different methods of adding magnesium have been developed, with the aim of giving predictable, high yields. Magnesium reacts with sulphur present in the liquid iron until the residual sulphur is about 0.01%. Until the sulphur is reduced to near this figure, the magnesium has little effect on the graphite formation. In the formation of MgS, 0.1%S requires 0.076%Mg. A measure of the true Mg recovery of the treatment process canbe expressed as:

$$\%\ \text{Mg Recovery} = \frac{0.76 * (\%\text{S in base metal} - \text{residual }\%\text{S}) + \text{residual }\%\ \text{Mg}}{\%\ \text{Mg added}}$$

Typical analysis of magnesium ferrosilicon nodulariser

Element	*5% MgFeSi*	*10% MgFeSi*
Si %	44-48	44-48
Mg %	5.5-6.6	9.0-10.0
Ca %	0.2-0.6	0.5 - 1.0
RE %	0.4-0.8	0.4 - 1.0
A1%	1.2 max	1.2 max

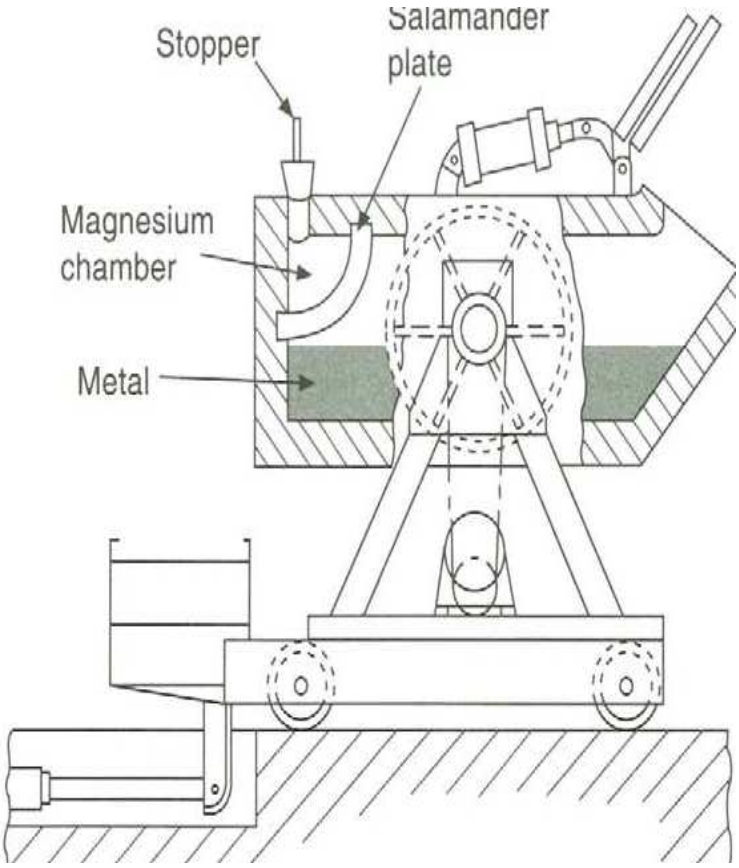

Fig 1.4 G.F. Fisher Method for production of ductile iron.

This method have advantages and disadvantages; simple treatment methods can only be used with the more costly low-Mg alloys, generally containing high silicon levels which can be a restriction since a low Si base iron must be used. In order to use high Mg alloys and pure Mg, expensive special purpose equipment is needed so the method tends to be used only by large foundries.[7]

1.7 Unique Properties of S.G. Iron: -

This member of family of cast iron has several interesting properties as:

- High strength (In some cases even greater than steel)
- Adequate Ductility.
- Superior cast ability (Foundry men friendly)
- Excellent machinability (As compared to steel)
- Lower density then that of steel
- Superior surface lubrication properties
- Better damping characteristics (As compared to the steel)

In addition, on the whole, S.G. iron has a reasonably good reliability. [8]

1.8 Matrix Structure Controls the Properties of Ductile Irons

These irons are cast after treatment of the molten metal with a small quantity of magnesium to change the graphite forms a flake to nodular or spheriodal form.Graphite nodules are small and constitute only small planes of weakness in the steel – like matrix, these being about one two – hundreth the size of those occurring when flake graphite is present. Because of this, and also because the graphite is spheroidal, stress concentrations round the graphite are small, and ductile irons have mechanical properties which relate directly to the strain and ductility of the matrix present as is the case for steels. Unlike gray cast irons, which generally fail with less than about one percentage elongation, ductile iron can deform plastically before fracture and have elongation of 2–25 %. Strengths generally decrease as the elongation increases. When high – strength matrix structures are obtained by heat treatment, such as normalizing, hardening and tempering,

and austempering, it is possible to produce irons with both increased strength and relatively high elongations.[1,3]

1.9 Effect of Alloying Elements on Matrix Structure of S.G. Iron. [5]

Element	Normal addition Level %	General effects of element
Silicon	1.5-2.5	Promotes ferrite but with peralitic matrices increasing silicon increased proof stress, hardness and tensile strength. Danger of embrittlement.
Manganese	0.3-1.0	Mild pearlite promoter. From intercellular carbides especially in heavy sections. Increases proof stress and hardness to a small extent. Danger of embrittlement.
Copper	0.5-2.0	Strong peatlite promoter. Increases proof stress, tensile strength and hardness with no embrittlement of matrix.
Nickel	0.5-2.0	Mild pearlite promoter increases proof stress but little effect on tensile strength. Danger of embrittlement with large additions in excess of about 2 %

Tin	0.05-0.1	Very strong pearlite promoter. Increases proof stress and hardness but danger of embrittlement giving low tensile strength/ elongation values
Molybdenum	0.2-1.0	Mild pearlite promoter. From intercellular carbides especially in heavy sections. Increases proof stress and hardness. Danger of embrittlement giving low tensile strength and elongation improves elevated temperature properties.
Arsenic	0.05-0.1	Very strong pearlite promoter. Not used commercially. Possible risks of embrittlement.
Antimony	0.01-0.05	Very strong pearlite promoter. Not used commercially in S.G. iron.
chromium	< 0.1	Very strong carbide former. Should not be employed if carbide – free structure is required.

1.10 Magnesium Vs Shrinkage

In Mg treated irons, high Mg content acts to promote carbidic microstructures and increase shrinkage. The magnesium level must be controlled carefully to the cooling rate of the casting to avoid increased chilling tendency. This cooling rate is described as proportional to the modulus, which is a ratio of casting volume to cooling surface area. Thus modulus is a more accurate away to describe the cooling of a casting section than just measuring the section size. Of course, all of the carbide stabilizing elements should be kept at relatively low levels to minimize their effect on chill formation. Doing this, will allow more of the available carbon to transform into graphite. [9]

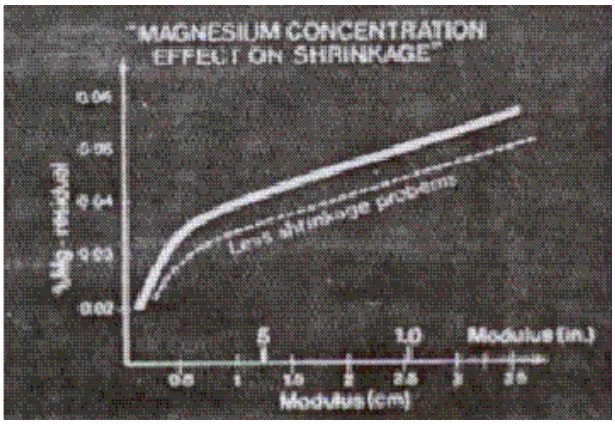

Fig 1.5Effect of Mg on shrinkage, [9]

1.11 Quality Index of S.G. Iron

Quality Index for ductile iron was developed in a statistical study of mechanical properties of a large no of Ductile Iron samples by Siefer and Orths who identified a relationship between tensile strength and Elongation in the form:

$$\textbf{(Tensile Strength)}^2 \textbf{ x (Elongation) = Q}$$

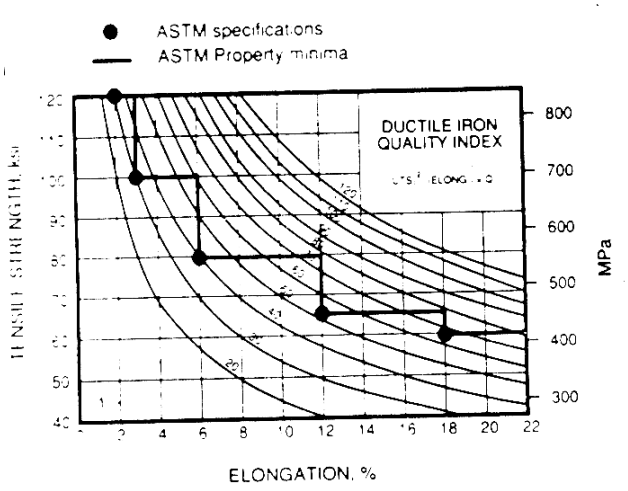

Fig 1.6

Where, Q is a constant and was later referred to as a Quality Index for Ductile Iron. A larger value of Q indicates a combination of higher Tensile Strength and / or Elongation or both and is therefore indicative of a higher level of material performan.High Q value irons have been shown to result from high nodularity, high nodule count, structures with an absence of intercellular degenerate graphite, free from carbides, low phosphorus (< 0.03 %) and free from porosity. Foundries seeking to optimize the fatigue strength of ductile iron castings need to produce high Q value material by taking actions to ensure ----

- Achieving maximum pearlite and matrix hardness.
- Achieving high nodularity, high nodule count and small size of nodule.
- Achieving inclusion free casting.
- Eliminating shrinkage porosity.
- Low levels of tramp and residual elements.
- Minimum carbide content.
- Free from dross defect.[4]

1.12 Ductile and Brittle Behavior Of S.G. Iron:

All ferrous materials, with the exception of the austenitic grades shows a transition from ductile to brittle behavior when tested above and below a certain temperature known as transition temperature. A comprehensive treatment of the subject by ***Barton*** has been used to identify and discuss some of the factors affecting Ductile and Brittle behavior as follows.

Ductile failure is accompanied by considerable general or local plastic deformation, usually shown by visible distortion of a failed component and by slow crack extension or tearing. A ductile fracture appears black in a fully ferritic ductile iron and gray in pearlitic irons. Ductile fractures occur by tearing from the sites of graphite nodules along grain boundaries. So that, the fracture contains numerous graphite nodules.

Brittle failure, by contrast, generally occurs without deformation, and very rapid crack propagation is involved. Brittle fractures in ductile irons are not associated with graphite sites and occur by cleavage of the metallic grains, usually before significant deformation has occurred. The separation through the grains very rapid and such fractures appears bright because the cleavage facets of the grains reflect light, a brittle fracture characteristically passes through the grains and very few, if any, graphite nodules are present along the fracture path. The transition temperature of a material is raised if loading speeds are high or if a notch is present. For this reason, brittle fractures are more commonly observed during impact testing then there during normal tensile testing. It is important to appreciate, however, that brittle failure can occur under normal tensile loading if the conditions favour this mode of failure. A simplified explanation for this ductile – to – brittle transition behavior is shown in figure 1.7, At higher temperatures, the stress required to cause plastic deformation is relatively low and failure occurs in a ductile manner, with considerable deformation, before the stress to trigger brittle failure by cleavage is exceeded. The stress required to cause plastic yielding increases rapidly as the temperature is decreased, and the stress required to produce brittle fracture may then be exceeded before plastic yielding can take place.[2,10]

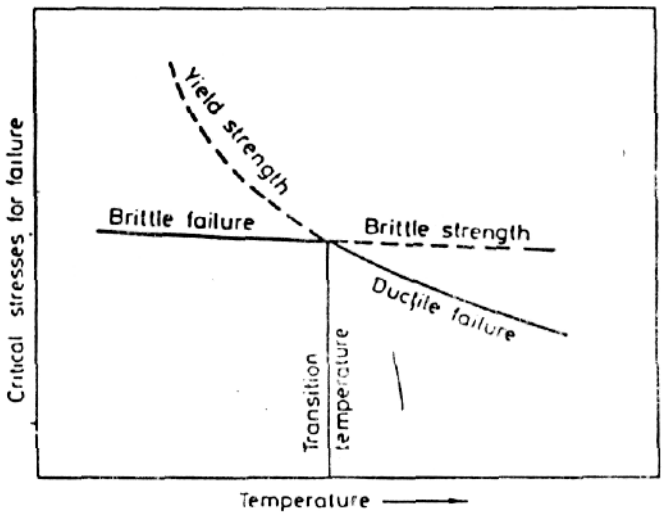

Fig 1.7: Ductile to Brittle transition occurs as temperature increases.[10]

1.13 Factors Affecting Tensile Properties Of S.G. Irons

1.13.1 Chemical Composition

In ferritic ductile irons, the effect of an increase in carbon is to increase the volume of graphite produced, which in turn reduces tensile strength, elongation and hardness. The strength properties of ferritic ductile irons are increased by the addition of elements that go into solid solution in ferrite. Silicon and Nickel are the most important elements to be considered.An increased Silicon content promotes ferrite and strengthens the ferritic matrix. When the Silicon content exceeds 4%, the ferritic matrix becomes sufficiently embrittled to give a lower tensile strength. In pearlitic ductile irons, Silicon promotes ferrite and helps prevent carbide formation. An increase in the Silicon content of pearlitic irons normally results in embrittlement of the pearlitic matrix with accompanying reductions in tensile strength and elongation, although proof strengths continue to increase.[2]

1.13.2 Temperature

Work at BCIRA has shown that the ductile – to – brittle transition in pearlitic ductile irons is evident in the tensile test by reductions in strength and elongation. The effects of increase in Silicon and Phosphorus on tensile strength and elongation over the temperature range + 100 to –300^{o}C are shown in figure 1.7. These results illustrate that Silicon and Phosphorus can embrittle pearlitic ductile irons and reduce tensile strength at room temperature, in the same way that they embrittle ferritic ductile irons, where the effect is normally observed in the notched impact test.[11]

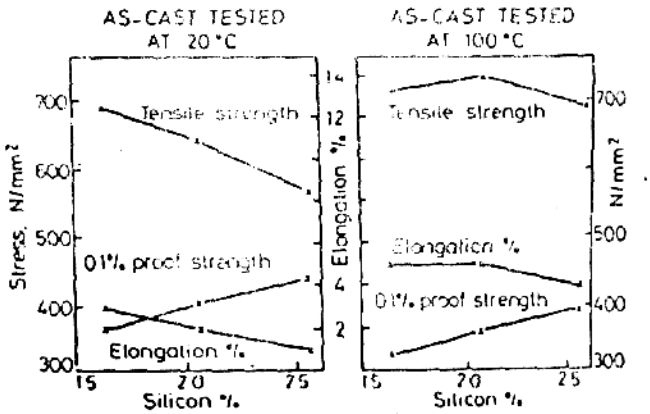

Fig 1.7: Effect of silicon content on the tensile properties of pearlitic ductile irons

1.13.3 Casting Soundness

Unsoundness in ductile irons can cause dramatic reductions in tensile and other mechanical properties. The factors, which affect the soundness of the castings, are follows:

- The type of mold material used.
- The rigidity of the mold.
- Design of the casting.
- Getting system employed.
- Composition of the iron.
- Thermal history of the metal processing, including Mg treatment temperature and inoculation.

The levels of carbon and silicon, particularly carbon, are important factors governing the soundness of ductile iron castings. The optimum range of carbon is 3.4 to 3.6 %. Above or below is dangerous for casting soundness. Above 3.6 % carbon, however a larger volume of graphite is precipitated during solidification resulting in higher pressure being exerted on the mold walls. Unless the mold was rigid enough to with stand these pressures then mold – wall movement will occur, increasing the casting volume and promotion unsoundness.[2.12]

1.14 Heat Treatment [13]

1.14.1 Annealing

Annealing, sometimes referred to as full annealing, is necessary for castings which are carbidic as – cast. The samples are hold at a temperature of 900^{o}C for 2hours and one additional hour per inch section thickness. Then, cool to 700^{o}C and hold there for 5 hrs. Finally, cool at a maximum rate of 110^{o}C per hour to 480^{o}C, then air cool.

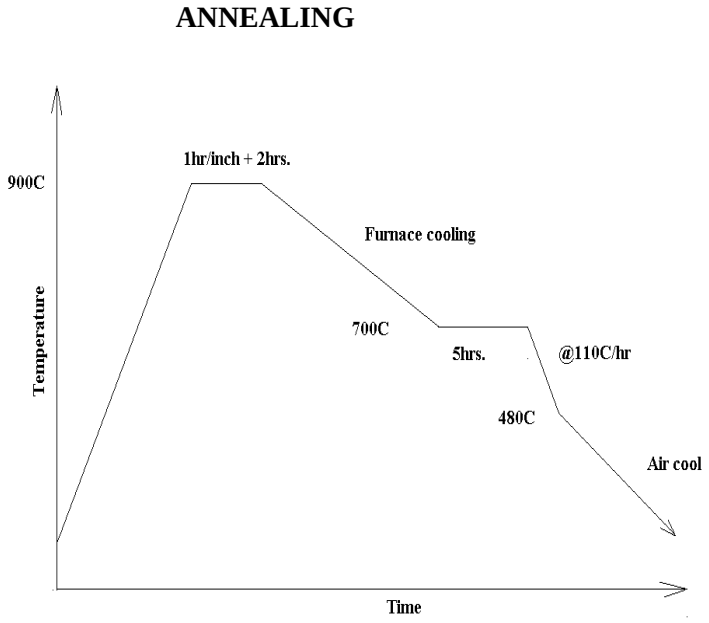

Fig 1.8: Annealing heat treatment

1.14.2 Normalizing

The result of normalizing is a fine pearlite matrix. Heat the casting to 900^{o}C, if massive carbides are present in the structure. Otherwise, heat to A_3 +83^{o}C. Then, hold for one hour plus one additional hour per inch section thickness. Remove the casting from the furnace and air – cool. Most ductile irons to be normalized are also alloyed with up to 1.5 % Cu or up to 0.075% Sn in order to promote a fully pearlitic matrix. The heavier the section the more alloying is needed. To increase hardness and strength Cu is mixed.

When Si content is more than 2.5%, the casting should be fast cooled to get a fully pearlitic matrix.

NORMALIZING

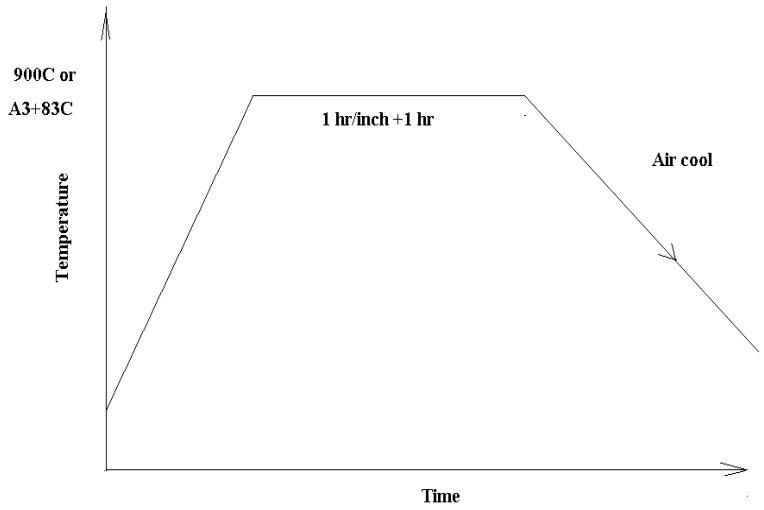

Fig 1.9: Normalizing Treatment

1.14.3 The Austempering Process

Austempered ductile iron is produced by heat-treating cast ductile iron to which small amounts of nickel, molybdenum, or copper have been added to improve hardenability. Specific properties are determined by the careful choice of heat treating parameters. Austempering involves the nucleation and growth of acicular ferrite within austenite, where carbon is rejected into the austenite. The resulting microstructure of acicular ferrite in carbon-enriched austenite is called ausferrite. Even though austenite in austempered ductile iron is thermodynamically stable, it can undergo strain-induced transformation to martensite when locally stressed. The result is islands of hard martensite that enhance wear properties.Advanced Cast Products uses salt baths for austenitizing, quenching, and austempering in order to achieve close dimensional control. Times and temperatures are tightly controlled throughout the entire process.

Steps in Austempering Process

1. Heat castings in a molten salt bath to austenitizing temperature.

2. Hold at austenitizing temperature to dissolve carbon in austenite.

3. Quench quickly to avoid pearlite.

4. Hold at austempering temperature in molten salt bath for isothermal transformation to ausferrite.[13]

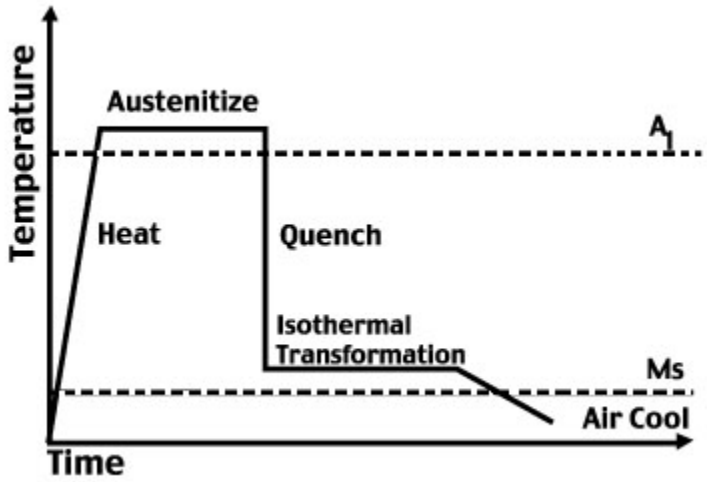

Fig 1.10: Austempering Procedure[13]

1. Initial austenitizing times and temperatures (1550° to 1700° F.) are controlled to ensure formation of fine grain austenite and uniform carbon content in the matrix. The precise temperature is grade dependant.

2. Quench time must be controlled within a few seconds, to avoid formation of pearlite around the carbon nodules, which would reduce mechanical properties. Quench temperatures (450° to 750° F.) must stay above the point of martensite formation (except for ASTM A 897 Grade 5).

3.In the austempering step which follows austenitizing, the temperature of the final salt bath must also be closely controlled. The austempering step is also precisely time-controlled, to avoid over- or under-processing. By the end of this step, the desired ADI ausferrite structure has developed.

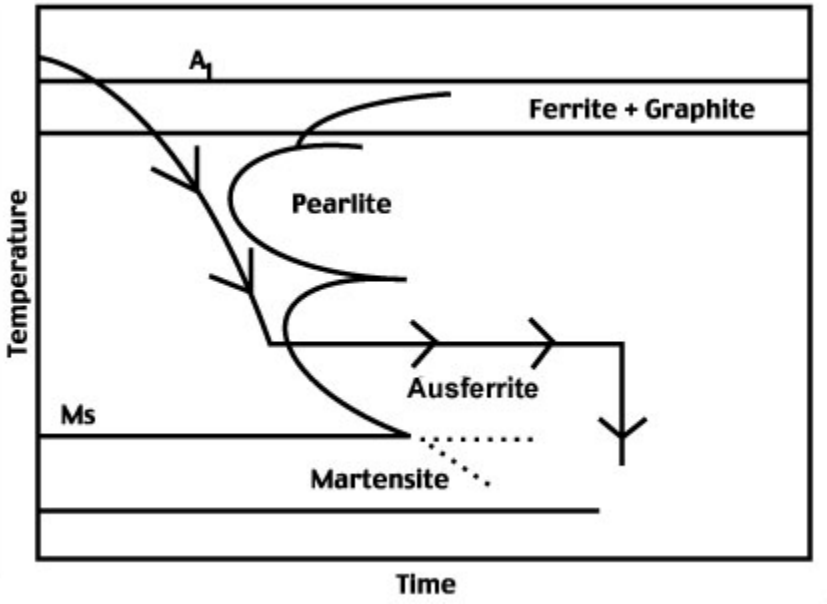

Fig1.11: Isothermal curve representing austempering process.[13]

1.15 Properties of ADI Compared to Steel [14]

- ADI is much easier to cast than steel
- ADI is approximately 9% lighter than steel
- ADI has minimal draft requirements compared with steel forgings
- ADI loses less of its toughness than steel at sub-zero temperatures
- ADI work hardens when stressed
- ADI has more damping capacity than steel

1.16 Applications Of S.G. Irons

The applications of the S.G. iron have increased tremendously in recent times as can be seen from the list below. [8]

- Engine crank shaft
- Brake caliper, disc – brake anchor, brake anchor plate
- Machine – tool bed
- Electric insulator post and cap
- Steering knuckle
- Rack and pinion of steering assembly
- Piston for impact drills
- Rolling mill rolls
- Moulding boxes and mould box clamps
- Brake shoe for heavy duty brakes
- Glass moulds
- Spacer cage for rolling bearing
- Piston rings
- Wind mill items

Following figure 1.12, compares the Tensile and elongation properties of austemperd ductile iron with other treated irons.

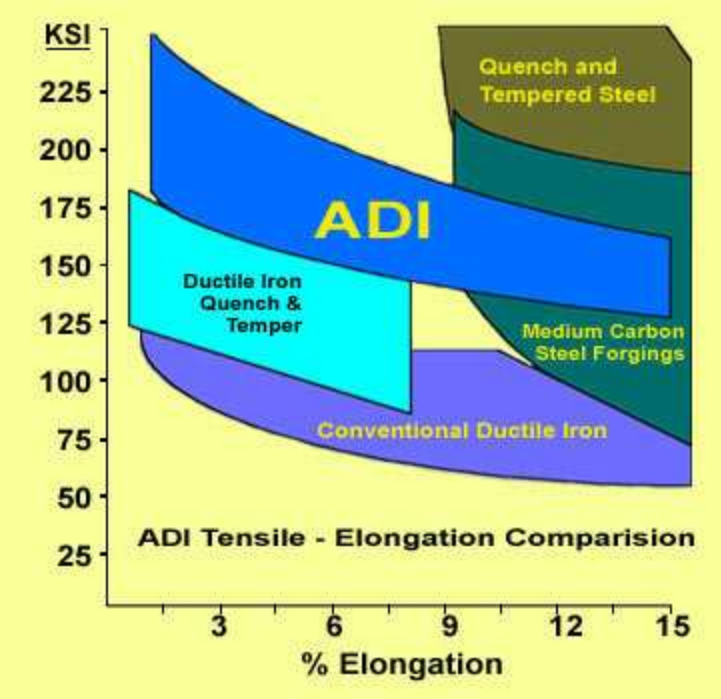

Fig 1.12: Comparision of ADI'S Mechanical properties withh other

treated irons

1.17The ADI Microstructure

Ductile Cast Iron undergoes a remarkable transformation when subjected to the austempering heat process. A new microstructure (ADI) results with capability superior to many traditional, high performance, ferrous and aluminium alloys. To optimise ADI properties for a particular application the austempering parameters must be carefully selected and controlled. Castings are first austenitised to dissolve carbon, then quenched rapidly to the austempering temperature to avoid the formation of deleterious pearlite or martensite. While the casting is held at the austempering temperature nucleation and growth of acicular ferrite occurs, accompanied by rejection of carbon into the austenite. The resulting microstructure, known as "Ausferrite", gives ADI its special attributes. Ausferrite exhibits twice the strength for a given level of ductility compared to the pearlitic, ferritic or martensitic structures formed by conventional heat treatments.

Because the carbon rich austenite phase is stable in Austempered Ductile Iron it enhances the bulk properties. Furthermore, while the austenite is thermodynamically stable, it can undergo a strain-induced transformation when locally stressed, producing islands of hard martensite that enhance wear properties. This behaviour contrasts with that of the metastable austenite retained in steels, which can transform to brittle martensite. [15]

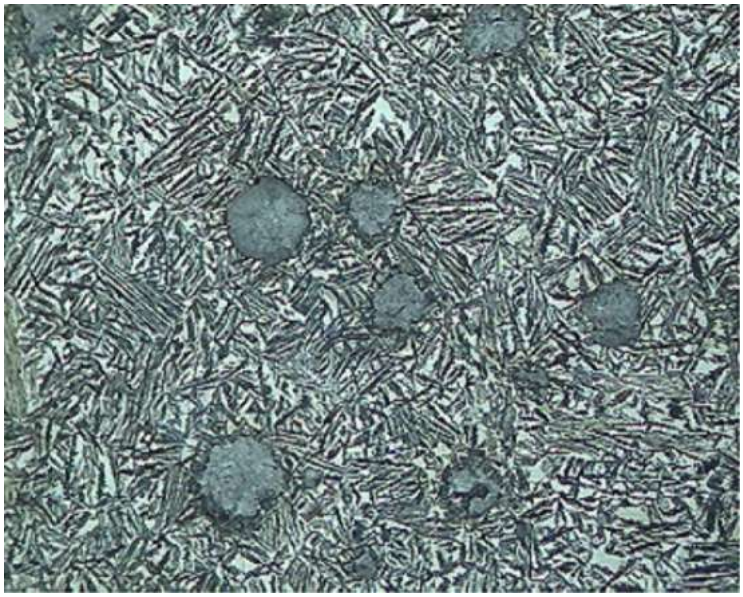

Fig 1.13: Microstructure of ADI

1.18 Applications Of ADI

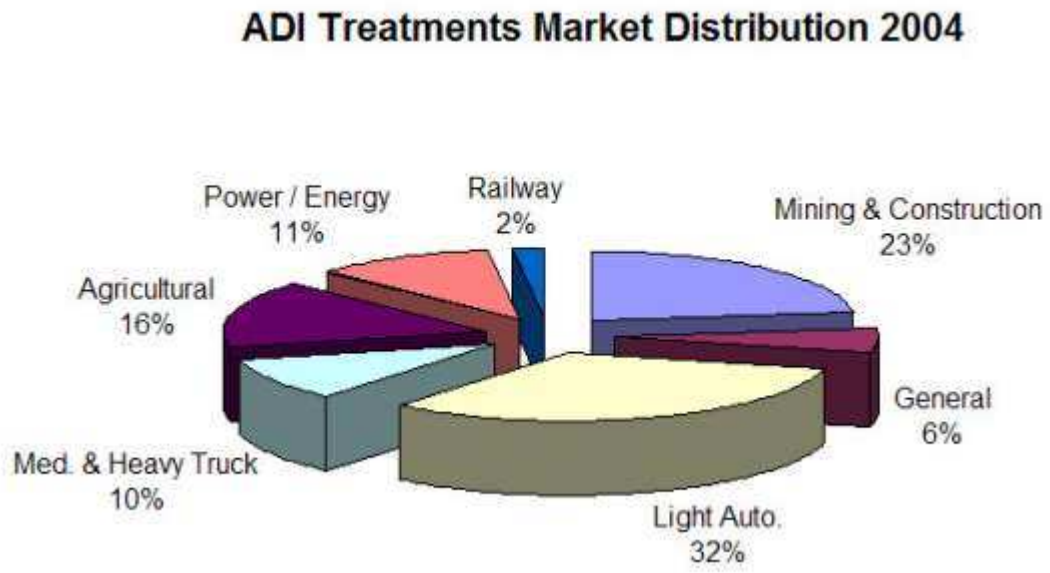

Fig 1.14: Application of ADI in different areas.[16]

Over twenty years, heat treatment specialists and equipment engineers have refined the Austempering process and plant to enable reliable production of high grade Austempered materials. This has fuelled demand and a family of Austempered Irons and Steels are now routinely produced. Of these **Austempered Ductile Iron** is increasingly the material of choice as designers and engineers seek cost effective performance from their components and systems. In particular, manufacturers engaged in moving parts and safety critical items have benefited from increased strength, greater wear resistance, noise reduction and weight saving.

ADI is now established in many major markets:

- Agricultural Equipment
- Construction Equipment
- Gears/Powertrain
- Heavy Truck/Trailers
- Light Vehicles and Buses

- Mining/Forestry Equipment
- Railway
- Farm and Oilfield Machinery
- Conveyor Equipment and Tooling
- Defence
- Energy Generation
- Sporting Goods

ADI is also finding new markets. In particular the burgeoning Renewable Energy field has identified ADI components to replace conventional materials solutions. Meanwhile specialist applications of the other Austempered cast irons (AGI, and CADI) are growing and there are niche markets for the unique Carbo- Austempering process.[16]

Objective of work:

The objective of this work is to determine the mechanical properties and microstructure of heat treated ductile iron with two different grades. One is with Cu and other is without Cu. After that compare these properties with different treatment conditions, the treatment conditions are mainly tempering at different temperature and austempering at constant temperature and variation of time. Mechanical properties are:

1. Tensile strength (U.T.S., 0.2% elongation),
2. % Elongation,

Then these mechanical properties are related with microstructure and fracture surfaces of the different samples after treatment.

CHAPTER 2

Literature Review

CHAPTER 2

2.1 Introduction:

From the available literature, it is quite evident that many attempts were made to understand and predict the behaviors of ductile iron that includes the study of graphite morphology and its evolution, the response of matrix structure to heat treatment, structure and properties correlation and its mechanical properties and possible application. A brief review of some literatures in this area is presented under here.

Literature Review

Ali M.Rashidi and M.Moshrefi-Torbati[17] have investigated the effect of tempering conditions on the mechanical properties of ductile iron with dual matrix structure. Tempering is the most important heat treatment process that was applied to quenched steel & cast iron. The objectives of this process include reducing the brittleness of the material, improvement of toughness & ductility and also reducing the probability of cracking. The composition of the material analyzed was (in Wt %) 3.56% C, 1.94% Si, 1.33%Ni, 0.28 %Mn, 0.29% Mo, 0.017%P, 0.012%S. In order to obtain a complete ferrite structure, the sample were first heat treated at 950˚C for 2 hrs. The samples were tempered at 300˚C, 400˚C, 450˚C, 500˚C, 600˚C for 1 hrs and also at 500˚C for 30, 90,120, 150& 180 min. Finally, the samples were machined down to standard dimension and then tension experiment was carried out. It was seen that by increasing the tempering temperature, there was a rise in elongation percentage, prior to the sudden jump that occurred within the range of 400-500 ˚C, followed by a slow & gradual increase. Therefore, if the aim is to achieve high toughness & ductility, the dual phase ductile ductile iron with ferrite-martensite matrix structure should be tempered at temperature higher than 500˚C.Again as the tempering temperature increased,the yield strength ultimate tensile strength initially decreased then within the range of 400-500˚C remained roughly constant and then there was a rise in elongation percentage for tempering upto 120 min before it is finally dropped. The reason for this reduction was likely to be due to a phenomena called temper embitterment. Within the temperature range of 400-500˚C, both strength and yield stress

decrease .Longer duration of tempering period at 500˚C increases the elongation percentage for tempering period upto 120 min reduces strength and yield stress, thereafter, they both go up again. For any combination of temperature of tempering and tempering period and of up to 120 min. the amount of ultimate tensile strength can satisfactorily be obtained from the master-curve's strength-tempering parameter.

O.I. Choi, J.Y.Kim, C.O.Choi[18], have studied the effect of rare earth elements on the micro structural formation and mechanical properties of thin all ductile iron casting. The amount of rare earth elements in the final casting were 0,0.02, 0.03 and 0.04% to observe the effect of the amount of RE on the formation of graphite nodules. Tensile testing specimen of various thicknesses was made and their tensile strength, yield strength, and elongation were measured using an Instron at cross speed of 1.5mm/min. Hardness tests were also performed on each sample using a Brinell Hardness tester. Average values of the hardness were obtained based on the 10 measurements. A 3000 kg load was applied to specimen with thickness of 4, 6,8 ,25 mm, and 500kg for 2 and 3 mm. The microstructure of samples were observed using a digital optical microscope (Leica-DMIRM HC) after polishing and etching using a nital solution. The number and size of the graphite nodules were recorded, and chill formation was also documented from optical photographs with 100 magnification. The graphite nodule count was determined by averaging the amount of nodule observed in 1 mm at 10 different locations. Micro structural features in thin wall ductile iron casting including the thickness of ferrite layer around the graphite nodules. Graphite nodule size, and graphite nodule count were observed to depend on the amount of rare earth elements and sample thickness. In the 2 mm thick specimen, the addition of RE led to a decrease in the amount of chill formation, a higher graphite nodule count and size as compared to those in the specimen without RE. However, the specimen whose thickness was in the range of 3-6 mm, the addition of RE led to a smaller graphite nodule size and a higher number of graphite nodules than those in the specimen without RE. These results suggested that the role of RE varies with sample thickness. In, addition chill formation was not obseverved in the samples thicker than 2 mm irrespective of the addition of RE suggested that the effect oof rare earth in reducing chill formation is important in very thin section. Thus it was concluded that nodulerty of graphite nodules improves due to the addition of RE. In the sample

without RE, the nodulerity increased with decreasing sample thickness; the RE addition significantly reduced the variation in nodulerity with sample thickness.

N.Fatahalla, S.bahi[19], have studied the metallurgical parameter, mechanical properties & mach inability of ductile cast iron. The material composition is 80% pig iron with 39% C & 0.9% Si, remaining 20% was returned S.G. iron with 3.6%C, 2.4%Si & 0.05%Mg.The chemical analysis has been done, for this material was melted in a high frequency induction furnace. The liquid metal was treated by Fe-Si-Mg alloy (45, 50 &5 mass %, 1.6% by wt of charge) having a grain size from 15 to 50 mm using a ladle sandwhich technique, then melt was inoculated by using Fe-Si alloy(20&80% by wt).Then ferritic heat treatment was performed using Gallen-Humb muffle furnace with maximum temperature of 1100˚C.They got that the nodule size ranged from 233 to 1368 nodule/mm2 for largest diameter in sand mould & smallest diameter in metal mould ingot. Nodulerity> 90% .The hardness test was also done by using Vickers hardness was found decreasing with increasing ingot diameter. There was a monotonic increase in ductility & decrease in strength was obdserved to occur with increase in ingot diameter. Tool life increases with increasing ingot diameter sand and metal moulds. Heat treated ingots both sand and mould have costant hardness. The tool life has changed due to variation of nodule characteristics.

H.Morrogh.[20], studied the influence of copper in ductile cast iron. He found that Cu appears to make the noduler iron more sensitive to the effect of subversive elements. up to 3%of Cu in the absence of subversive elements good noduler structures. If Ni is present in amount 5-20% with the presence of subversive elements then the cupper which is tolerated in presence of subversive elements can be increased, & the harmful effect of Cu can be neutralized by the addition of Ce. The mechanical properties noduler cast iron increased if the amount Cu is increased upto a certain level. The noduler iron which has no Cu had a matrix of 95% ferrite and 5% pearlite. The iron which has 0.27% of Cu had 50% ferrite and 50 % pearlitic structure. 3% Cu had no harmful effects on the noduler graphite formation. The cast iron which has 0.04% Ti

without Cu has almost graphite structure with trace of a flake form of graphite in matrix of pearlite. Ti gives the small amount of flake form of graphite in a matrix of pearlite with spherulitic nodules. The presence of 0.04% Ti with 1 % Cu is sufficient to interfere with the formation of noduler graphite. For Cu base alloy containing 25-40% magnesium and 1-6% Cerium is used to avoid from danger of Cu addition.

L.C. Chang, I.C Hsui [21], have studied and analyzed the erosion behavior of ductile iron. The chemical composition of the experimental material was Fe- 3.53%, C-2.88%, Si-0.11%, Mn 0.039%,P-0.011%, S-0.046%. The samples were austenized at 950˚C for 1 hr, and then water quenched to generate martensitic microstructure. Upper and lower bainite structure were obtained by quickly transferring samples from furnace after austenisation into an austempering bath preset at 420 and 280˚C for 1 hr respectively. The spherodial graphite cast iron samples after the above heat treatments were mechanically polished with the 800 grit size paper to remove surface scales. The samples were then subjected to erosion wear tests. The erosion rate was an average of at least three test results, which were taken as the weight loss per 500gm of the impacted SiO2 particles with the test time of about 8 min. Short term erosion test were also conducted to characterize the wear mechanism. The specimen for short term erosion were pre polished and slightly pre etched in 3% natal and eroded by a total of 1 gm SiO2 particles. The results of erosion test of ductile iron with four different matrices indicated that, the erosion rate first increases and then decreases with impact angle, a typical ductile behaviour of ductile iron. All four ductile iron exhibited similar erosion rate at the impact angle less than 30˚ apart fact that soft ferritic ductile iron showed a somewhat higher erosion rate at 15˚. Short term erosion test reveled that cooling is effective in both soft ferritc as well as hardness martensitic ductile iron with ferrite followed by those with upper bainite, lower bainite and martensite. Increasing hardness was seen to incur increasing with impact angle, while that of erosion rate/elongation showed showed an inverse trend.

Olivir. Ericet.al.[22] Investigates the austermping study of alloyed ductile iron. The ductile iron alloyed with 0.45% Cu and austempered at different time and temperatures range. After this the effect of this heat treatment on the microstructure and mechanical properties of ADI was analyzed. The chemical composition of the sample in wt % was 3.6%C, 2.5% Si, 0.28 % Mn,

0.45% Cu rest were other elements. The austempering temperatures and times after austenisation were 300° C, 350° C and 400 °C for 1hrs, 2hrs, 3h hrs and 4hrs respectively and then air cooled to room temperature. They found that that specimen austempered at 300°C for 2 hrs consists of banitic ferrite retained austenite and some amount of martensite. The specimen austempered at 300°C for 2hrs shows a typical lower bainite structure with acicular bainitic ferrite structure. The sample at 350°C for 2hrs shows a acicular appearance of bainite ferrite in a matrix of retained austenite. There was a plate like bainitic ferrite at higher temperature and martensite disappears. The fracture surface of impact tested surface shows a fully brittle fracture at 300°C. The samples austempered at 300° C, 350° C, 400 °C for 2 hrs shows the mixture of ductile and brittle fracture, but at 400°C the completely ductile fracture converts into cleavage brittle fracture. The strength remains unchanged till 3hrs and after that for 300°C and 350°C the strength increases. There was a maximum elongation and impact energy after 2 hrs because of disappearance of martensite and increment in bainite ferrite and retained austenite. With further increase of time there was a decrease in both elongation and impact energy and it is specially occurs at 400°C.The variation of 0.2% proof stress, U.T.S, elongation and impact energy after 2 hrs is also studied and they found that at lower temperature high strength is associated because of an acicular appearance of bainitic ferrite with some martensite and retained austenite. At 350°C there was a highest amount of retained austenite at which the elongation and impact energy have maximum value. So the temperature 350°C at 2 hrs is the optimal processing window at which UTS was 180MPa, elongation 8%, impact energy 160 J, and the fracture mode was fully ductile. By comparing these values with without Cu, ADI shows that Cu decreases strength but increases elongation and impact energy.

Sushil K. Putatundaet.al. [23] Investigation was to create the Austenite Free Austempered Ductile Cast Iron or completely ferrite matrix ductile iron. In this work the tempering is done after austempering treatment and the physical and mechanical properties were compared with austempered ductile cast iron. The chemical composition of the ductile iron was C 3.45%, Cu 0.3%, Si 2.48%, Ni 1.5% and rest were other elements. Two batches of samples were prepared; one batch of samples was processed by conventional austempering treatment. The second batch was tempered at 484°C for 2hrs after austempering treatment. Finally these samples were air cooled to room temperature. After these treatment different properties as tensile test,

metallography and X-Ray diffraction, hardness and fractography were measured and analyzed. At the lower austempering temperature (260°C) the microstructure was needle shaped ferrite with bright etching austenite in which graphite nodules were dispersed. On, the other hand theat higher temperature (385°C) coarse and feathery ferrite characteristic of upper banitie was observed. The samples which were additionally tempered at 484°C after austempering shows totally ferritic microstructure. The X-Ray diffraction profile of non-tempered samples shows both ferrite and austenite peaks, while the additional tempered samples shows only ferrite planes at an angle 42° to 46° and at 72° to 92°. This indicates that after tempering only ferritr present in these samples and austenite was below the resolution of X-Ray. The hardness of non-tempered samples decreases as the temperature was increased. On the other hand the hardness of the tempered samples at 500°F and 600°F had much lower value than that of non-tempered samples, whereas at 725°F had higher than that of the non-tempered samples. The yield strength of non – tempered samples decreases as the temperature increases from 260° to 385°C. When the yield strength of tempered samples was compared with non-tempered samples there was no significant difference, but when ductility of these samples were compared then they found that there was significant decrease in ductility for the temperature 316°C and 385° C. For the austempered samples at 260°C there was no decrease in ductility. The fracture surface of non-tempered samples shows a mixed mode of fracture with cleavage and few dimples. The fracture surface of tempered samples (austempered at 385°C) shows a cleavage type of fracture, while there was not much difference in the appearance of the fracture surface at 260°C tempered and non tempered samples.

P.W. Shelton, A.A. Bonner [24], in this paper describes the effect on the mechanical properties of elemental copper additions (above the levels of solid solubility), to a commercial ADI composition and micro structural studies are used to determine the distribution of the copper. Two types of compositions were prepared with different compositions. The composition of first and second sample were C 3.5%, Si 2.5%, Cu 1.5%, Mo 0.4% and C 3.5%, Si 2.5%, Cu 0.8%, Mo 0.73% and rest were other elements. Specimens were austenitised in batches at 900 and 940 °C. After a holding time of 2 h, the specimens were quenched into a salt bath at 270°C, 290°C,320°C and 350 °C for 2 h then air cooled to room temperature. Microstructure shows that

closer examination revealed small islands of copper or a copper-rich phase within and around some of the graphite nodules and some occasional small areas of copper within the ausferrite matrix. In some cases the copper is associate with the graphite nodules, but not necessarily as a thin film. There were also isolated pools of copper present in the microstructure. Hardness and strength of the ADI were adversely affected by the addition of Cu. The plain ADI has a higher hardness than the copper enriched ADI at the lower austempering temperatures, at the higher temperatures, the hardness converge. Lower austempering temperatures yield a finer structure and therefore higher hardness. The difference in hardness was reflected in the tensile strengths, the copper enriched material being lower than the plain ADI, though there was no difference at the higher austempering temperature. All the samples show the limited ductility of the order of 1–3%. Fracture surfaces showed evidence of micro-cracks running into the fracture surface between graphite nodules. The fracture toughness behaviour of both materials is almost identical and responds in the same way with increasing austempering temperature.

Kadir Kocapete et al.[25], studied the tensile fracture behaviour of oil quenched from intercritical annealing temperature (ICAT) range ($\alpha + \gamma$) and then tempered ferritic ductile iron having dual matrix structure (proeutectoid ferrite + martensite) with different martensite volume fraction and its morphologies have been studied for a ductile ferritic cast iron. The chemical composition of ductile iron is c 3.5%, Cu 0.005%, Si 2.63%, Mn 0.318% and rest are others. As cast samples were also heat-treated at the conventional austenitizing temperature of 900°C in single-phase region of Fe–C–Si equilibrium phase diagram and then quenched into oil and tempering was also done for comparision with other treatments. As cast material had ferrite+ graphite structure Oil quenching produced a microstructure that was nearly wholly martensitic were intercritically annealed at various temperatures of 795, and 815 °C for 30 s and then quenched into oil held at 100 °C to obtain different martensite volume fractions. The quenched samples were further tempered at 550 °C for various times from 1 to 3 h. The tensile test, microstructure and fracture surface examination was done after these treatments. They found that the elongation of ductile iron with dual matrix structure is comparable with that of ductile iron with ferritic matrix. It is also superior to that ductile iron having a fully martensite structure (conventionally quenched + tempered ductile iron). With increasing the MVF the fracture pattern

changed from ductile to brittle fracture. In the case of increasing continuity of martensite structure, fracture pattern changed from ductile to moderate ductile nature. Fractographic examination showed that ductile iron with dual matrix structure fails in a ductile fashion.On the other hand, in the conventionally heat treated samples with fully martensitic structure fracture mode is typical brittle fracture. Tensile strength and 0.2% proof stress was maximum for the sample which was conventionally heat treated and then quenched, but elongation was minimum in that case. While for as cast samples these strength was minimum and was maximum.

Mahmud Hafiz [26], studied the mechanical properties of spheroidal graphite (SG)-iron subjected to variable and isothermal austempering temperatures heat treatment. Variable austempering temperature heat treatment is carried out by austenitizing at 1183 K then quenching into a salt bath held at 593 and 723 K, respectively. After quenching, the former is steadily heated to 723 K while the latter is allowed to cool progressively to 593 K. The tensile properties, impact toughness and hardness are determined and correlated with the microstructure. Chemical composition of samples was C 3.5%, Si 2.54%, Cu 0.018%, S and P 0.007% and rest was Fe. The microstructure of the as-cast SG-iron is typical bull's eye structure. This structure has a non-homogeneous matrix due to the presence of varying amounts of ferrite and pearlite. Consequently, total combined carbon in the matrix is not uniform throughout the matrix. To get a uniform matrix structure, SG-iron is annealed and the resulting matrix structure is fully ferritic Two groups of experiments have been carried out for this.In the first one, specimens are austenitized at 1183 K for 3.6 ks, then austempered at constant temperatures namely 593 and 723 K, respectively, for 5.4 ks followed by cooling in still air to 300 K. The microstructure study shows the at austempering temperature 593° K very fine needles of ferrite are observed with a small amount ofretained austenite in between. As the temperature is raised to 723 K, the amount of austenite is increased.Increasing the austempering temperature is also found to result in coarse ferritic needles ferrite isolated from each other by austenite-regions the microstructure in that case consists of a mixture of upper and lower ausferrite. In the specimens quenched from austenitizing temperature of 1183 to 723 K and cooled progressively over a 3.6 ks period to 593 K have a microstructure consists of widely spaced ferrite and retained austenite. The microstructure of specimens quenched from 1183 K into a salt bath held at 593 K and heated to 723 K over a 2.7 ks .This structure contains a mixture of lower and upper ausferrite. The tensile

properties of specimens quenched at 593 K and heated steadily to 723 K, have higher 0.2% yield stress and ultimate tensile strength but much less ductility than those quenched at 723 K and cooled progressively to 593 K. It can also be noted that the 0.2% yield stress and the ultimate tensile strength are slightly lower than those of specimens quenched at the same temperature but isothermally held for 5.4 ks. However the elongation of the former is about three times of the latter. While specimens quenched at 723 K and steadily cooled to 593 K showed a 0.2% yield stress and an ultimate tensile strength slightly lower than those of specimens quenched and isothermally austempered at 723 K. However, the elongation is almost the same under both austempering conditions. the specimens quenched at 593 K and heated steadily to 723 K display higher impact toughness than those quenched at 723 K and cooled progressively to 593 K. the hardness of specimens quenched at 593 K and steadily heated to 723 K is lower than that quenched at the same temperature and austempered isothermally. The fracture surfaces off different heat treated samples were investigated also. Specimen austempered isothermally at 593 K for 5.4 ks, shallow dimples and cleavage fracture pattern could be observed. On the other hand, fine dimples and less areas of cleavage fracture are the characteristics of specimens austempered isothermally at 723 K for 5.4ks. The fracture surface of specimen quenched at 593 K and heated progressively to 723 K shows fine dimples near the graphite nodules and a quasi cleavage pattern of fracture in areas far from the graphite nodules. A wide and deep dimple pattern of fracture reflecting the high ductility and toughness of the specimen quenched at 723 K and cooled steadily to 593 K.

Olivia Eric, Dragan rajnovic et. al. [27] have studied the microstructure and fracture of alloyed ductile iron. The microstructure and fracture mode developed through these treatments have been identified by means of light and scanning electron microscopy and X- ray diffraction analysis. They studied the microstructures by light micrograph and found that the microstructure of the ADI alloyed with Cu was pearlite, at 70vol. %, and the ferrite (30vol.%) and the mainly spherical graphite nodules. The microstructure of the ADI alloyed with Cu+ Ni consists of graphite spheroid nodules in a fully pearlitic matrix. The microstructures of the ADI alloyed with Cu and austempered at 350°C for 1, 2 and 6h were also studied. Samples for 1 hr shows the predominant phase is martensite, whereas only small amounts of acicular ferrite (lower bainite) and retained austenite and for 2 hrs martensite could not be detected and the structure consisted

only of acicular bainitic ferrite and retained austenite. During longer austempering (6h), the amount of retained austenite decreases and acicular bainitic ferrite dominates the microstructure. A small fraction of martensite is also present. Microstructures of ADI alloyed with Cu +Ni austempered at 350°C for 1, 3 and 6h were shown. After austempering for 1h, the microstructure reveals blocky darkened areas containing a high fraction of plate-like martensite with a low fraction of austenite. After 3h of austempering, there is an appreciable decrease in the amount of martensite and an increase in the amount of acicular bainitic ferrite and retained blocky austenite. After austempering for 6h, only small amounts of martensite and retained austenite are present in the microstructure. Comparing the austempered microstructures of both ductile irons they could observe that alloying with Cu +Ni promotes the transformation of upper bainitic ferrite. the X-ray diffraction patterns of ADI alloyed with Cu and Cu+Ni for different austempering times shows the profile of the 111 and 110 lines of austenite and ferrite were identified in nearly all cases. Diffractograms of ADI alloyed with Cu show that the intensity maximum of the 111 line was reached after austempering for 2h, whereas the presence of ferrite and martensite dominate after 1 and 6h. The situation is similar with ADI alloyed with Cu +Ni, except that the 111 line could not be detected after the shortest austempering time. The presence of a broad 110 line suggests that ferrite and martensite are the main microconstituents. The variation of retained austenite content with austempering time in both ductile irons was show that the variation of the volume fraction of retained austenite with austempering time is similar for both materials. The maximum value of retained austenite (16.5vol.%) noted in the ADI alloyed with Cu is achieved after 2h. However, with the ADI alloyed with Cu +Ni, the retained austenite reaches a maximum (19vol.%) after 3h. The impact energy increases as the austempering time increases up to a maximum value after which it decreases. ADI alloyed with Cu was achieved after austempering for 2h, whereas alloying with Cu +Ni the maximum to 3hr.By the analysis of fracture surfaces they observed that in the ADI alloyed with Cu a mixture of ductile and cleavage fracture prevails but in the Cu +Ni alloyed ADI only cleavage fracture can be seen after 6hrs, while for 2 and 3 hrs higher number of dimples observed .

Yon Jon Kim et. al. [28] investigates the mechanical properties of austempered ductile iron with austempering temperatures. Chemical compositions of two samples were close to each other as in one sample C 3.53%, Si 2.67%, Cu0.87%, Mo 0.25% rest are other and in second sample C

3.6%, Si 2.69% and rest are same. Each sample was austenitized at 910 °C for 90 min and transferred into a salt pot for tempering heat treatment in which the temperature varied from 350 to 410 °C in intervals of 20 °C. samples were soaked at those temperatures for 90 min. Microstructure of as cast samples contains ferrite and pearlite matrix with graphite nodules dispersed in it and after austempering heat treatment, the entire matrix was transformed to plate like shaped ausferrite structure. The mechanical properties of as cast samples were lower than the austempered samples. The as-cast sample shows an ultimate tensile strength (UTS) of 654 MPa with 4% elongation and 230 in Brinell hardness (HB). Austempered samples were found to be higher UTS and hardness as tempering temperature was decreased and the elongation was seen to be proportional to the tempering temperature. For austempered cast irons, brittleness was increased as austempering temperature went down. ADIs can possess more ductility but smaller increase in strength and hardness than transformed at lower bainite temperature ranges. In this study, copper and molybdenum were alloyed expecting suppression of pearlite formation as well as promotion of hardenability. The highest ductility was obtained from 410 °C austempered samples. However, the tensile strength was highest for 350 °C austempered cast iron. So Copper and molybdenum addition plays effective role in the formation of ausferrite structure as well as increment of mechanical properties such as tensile strength and hardenability.

Gulcan Toktaş et al.[29], studied the influence of the matrix structure on the mechanical properties and impact toughness. Chemical composition of sample is C 3.6%, Si 2.29%, P 0.053%, S 0.011%, Mn 0.08% and Fe is balanced. The cast ingots are divided into five groups in this work. The material in the first group is used directly or without any additional heat treatment (i.e. as-cast). For the second group the materialis subjected to ferritic heat treatment. The ferritization procedure followed the usual two stage isothermal holding, in which SG-iron is held at 1193 K for 18 ks, furnace cooled to 993 K for the second isothermal holding for 25.2 ks, and then furnace cooled to room temperature (»300 K). The materials of the remaining groups are heated to 1193 K, held for 18 ks at this temperature, then cooled to room temperature following different cooling rates, as in still air cooled, forced air cooled and cooled in an isolated block. Microstructure of ferrtic heat treatment shows the graphite nodules embedded in the fully ferritic matrix. The microstructure of ferrite-pearlite matrix with graphite nodules in the as-cast condition shows typical “bull’s eye” in which many of the graphite nodules are surrounded by an

envelope of ferrite. Both the graphite nodules and their ferrite envelopes are embedded in a pearlitic matrix. While the microstructure was same in forced air and in still air but pearlite to ferrite ratio was increased in latter case and there ferrite imbedded in pearlite. This ferrite formed without any particular relation to the graphite nodules. The tensile properties vary mainly through the influence of the pearlite content of the matrix.The 0.2% yield strength ranges from 240 MPa for ferritic to 457 MPa for pearlitic matrix SG-iron. The ultimate tensile strength (UTS) of the present material is also increased due to the increase of pearlite level. Compared to the fully ferritic matrix material, the percentage increase of the UTS is found to be about 25% in a ferritic /pearlitic matrix. The ferritic matrix shows the higher ducility then the pearlitic matrix SG-Iron. SG-iron with ferrite matrix exhibits the highest fracture energy, while with increasing percentage of pearlite, have lower fracture energy. The hardness value increases sharply as the matrix structure approaches a fully pearlitic condition. The fractrography shows that in a ferritic-pearlitic matrix structure material the fracture is traveling along a path that connects as many as possible graphite spheroids. It avoids the pearlite structure as much as possible. The fracture surface of ferritic SG-Iron shows the dimple pattern of fracture. Two different fracture patterns were observed in a ferritic-pearlitic matrix structure, in the vicinity of the graphite nodules, the wider areas of the ferrite phase are deformed considerably. Thus the fracture occurs in a ductile manner, while the brittle fracture with river pattern in pearlitic areas can be observed.

U. Ritha Kumari and P. Prasad Rao,[30], investigates the influence of austempering temperature on microstructural parameters and the wear behaviour of austempered ductile iron.The chemical composition of sample was C 3.5 wt%, Si 2.5 wt% ,Mn 0.3% ,S 0.1 wt%, P 0.02wt %, Ni 1.5wt%, Mo 0.3wt%, Cu 0.5wt %. For heat treatment all the samples were austenitised at 900 °C for 30 minutes and then austempered at a selected temperature for 2 h. Then seven different temperatures were selected for austempering as 260, 280, 300, 320, 350, 380 and 400 °C. By the microstructures analysis they observed that at lower temperatures of 260– 320 °C, the microstructure consisted of very fine ferrite needles with thin layers of austenite in between them and at higher austempering temperatures of 350–400 °C, the microstructure consisted of very coarse and feathery ferrite with relatively large amount of bulky austenite. At the highest temperature of 400 °C, coarse ferrite well separated from each other by wide areas of austenite. The quantitative information of microstructure was obtained by XRD-

technique. It was observed that the volume fraction of the austenite increased steadily from 15 to 41% as the austempering temperature was increased from 260 °C to 400 °C. The carbon content was very low, about 1.16wt%, when thesample was austempered at a low temperature of 260 °C. This rapidly rose to nearly 1.7 wt% when austempered at 300 °C. Beyond this temperature, the carbon content decreased slightly and reached a constant value with increasing temperature. Hardness is higher at lower austempering temperature and decreases as the austmpering temperature was increased. The tensile strength and yield strength were found to decrease monotonically as austempering temperature was increased. It was observed that the low austempering temperatures resulted in ADI of high strength and low ductility, while the high austempering temperatures resulted in ADI of low strength and high ductility. Wear rate increased with increasing austempering temperature. Formation of strain induced martensite during wear process has a considerable influence on the wear behavior. wear rate is inversely proportional to the yield strength of the ADI. High hardness and high strength which occurs at low austempering temperatures (260-300°C) leads to a very good wear resistance.

M. Cavallini et. al.[31], have studied the damage mechanism in the cast ductile iron. The chemical composition of the materials investigated were C 3.4 – 3.8%, Si 2.0-2.7%, Mn 0.3- 0.6 % and rest were other elements. For the microstructure examination the materials were mechanically polished and etched in the 2% nital solution. The original microstructure and microstructural features of theh damage regions near the fracture surface were observed using optical microscope and S.E.M.(to determine the fracture mode).The optical micrograph revealed the typical “bull’s eye” structure of graphite nodules surrounded by ferrite matrix of pearlite. The micrograph for theh fracture surface for the single edged notch beam specimens showed that, the crack initiates at the interface between the graphite and surrounding ferrite. The crack propagates following the graphite nodules path. The crack were arrested at the ductile ferrite that surrounds the graphite nodules, thus absorbing energy and leads to high fracture toughness. The fracture surface presents the different features i.e. i) graphite particles (which deboned from the surrounding matrix), ii) Cleavage region (which resulted from the failure of pearlite), iii) ductile dimples, primarily surrounded the graphite particles, which corresponds to the ductile damage in the ferrite. Thus the ferrite around the graphite nodules was most likely to be the main

contributor to the fracture resistance of the ductile iron, since it failed in the ductile manner that arrested the crack and absorbed the energy.

B.Stokes et. al.[32], investigates the Effect of graphite nodules on crack growth behavior of austempered ductile iron because it is an important material for camshafts, where the early stages of fatigue damage are of major concern during service. An ADI with composition 3.7C, 1.5 Si, 0.3 Mn, 1.0 Cu, 0.5 Mo in weight percentage and balance Fe was used. This was austenitised at 900 °C for 1h and austempered at 390 °C for 2 h. The microstructure study shows that the microstructure consists of coarse bainite laths, large blocky pools of retained austenite and graphite nodule embedded in it. During the austempering, the nucleation of bainite occurs at the graphite/austenite interface and grows by sympathetic nucleation of further plates into the austenite. At the same time, the growing bainite rejects carbon into the austenite. Due to the growth of bainite sheaves away from the graphite, these regions of supersaturated austenite exist in areas remote from nodules. Hence, for a conventional ADI alloy, as the distance from the graphite nodules increases, the proportion of austenite increases. Here thirteen short fatigue crack tests have been conducted within the 500–1100MPa maximum applied stress testing range. Failure in material occurred at approximately 28,000, 46,300 and 70,200 cycles for R = 0.1 and no failure occurred when a specimen was tested at a maximum stress of 500MPa with an R-ratio of 0.1. For R = 0.5 tests with a maximum applied stress of 1100MP failure occurred at approximately 32,000–43,000 cycle. The fatigue cracks initiation occurred exclusively at pores which were present either on the surface or immediately below the surface. Decohesion of graphite nodules and subsequent initiation and growth of micro-cracks may lead to deflection of the dominant crack system. It was also shown that there is a significant increase in the frequency of graphite nodules along the crack path as the applied stress levels were increased and further initiation events (confined to graphite nodules within the crack tip monotonic plasticzone) for crack occurred ahead of the propagating dominant crack tip throughout the lifetime of the specimen. So the changes in the as-cast microstructure generated by this heat treatment had resulted an improved fatigue crack propagation performance. This is due to the lack of eutectic carbides and the relatively high quantity of retained austenite in the microstructure.

A. Kutsov. et al.[33] studied the formation of bainite in ductile iron. The kinetics of bainite transformation under isothermal conditions was measured by conventional dilatometry. The results of these experiments show that there were two C-shaped curves, which correspond to the formation of upper bainite (500–390°C) and lower bainite (390–250°C), on the TTT diagram. Optical microscopy shows that how the morphology of the bainite changes from feathery-like in the upper temperature range to plate-like in the lower one. The chemical composition of material in this work was 3.2% C, 2.4% Si, 0.21% Mn, 0.59% Ni, 0.62% Cu, and 0.13% Mo (wt.) were used. The specimens were austenitized in the dilatometer under an Ar protective atmosphere at 950°C for 45 min, and then they were quenched into a lead bath at temperatures from 500 to 250°C. The elongation of the specimens was continuously monitored during the holdings in order to study the kinetics of the bainite formation. After that the specimens were cooled down to room temperature in the dilatometer. X-ray scans were performed with the DRON 3M diffractometer using Fe Kα radiation. The total volume fraction of the retained austenite was measured from the integral intensity of the (111) γ and (011)γ peaks. The results of the dilatometrical measurements for ductile iron are summarized in the form of a time-temperature-transformation (TTT) diagram. The TTT diagram shows that the temperature range of the bainitic reaction consists of two intervals 500–390 and 390–250°C. The first interval corresponds to upper bainite and the second one corresponds to lower bainite. The significant peculiarity of the bainitic transformation in this ductile iron was the existence of two minimal incubation times at 450°C in the upper temperature range and at 360°C in the lower temperature interval. At 450°C the transformation from the γ-phase to the bainitic α-phase ceased after 1100 s. The further holding causes the transformation to another phase starting after 3000 s which were carbide precipitation. The shape change associated with the formation of bainite is accommodated by dislocation slip in the parent austenite at upper temperatures and by twinning of the parent austenite at lower temperatures. By this it could be presumed that the kinetical and morphological peculiarities of bainite in the studied ductile iron are the result of different crystallographic shears during the formation of upper and lower bainite. By X-Ray measurement it was shown that as the isothermal temperature decreases within an interval of 500–250°C leads to a higher concentration of carbon trapped in the bainitic a-phase at the termination of the isothermal transformation. The decrease of the transformation temperature within an interval of 400–250°C causes a lower volume fraction of austenite (from 33 to 18%) to be retained in the

material as the transformation ceases. A comparison of the dilatometrical data with the X-ray results shows that the bainite transformation ceases once the carbon concentration in low carbon austenite reaches a certain value.

Ayman H. Elsayed [34],et.al. characterize mainly fracture toughness as well as the other mechanical properties of austempered ductile iron produced using both single-step and two-step austempering processes and also the effect of alloying with Ni and Mo has been investigated. In this study they used he two groups of samples. In one group the chemical composition was C 3.8%, Si 2.650 %, Mn 0.258%,P 0.037%, Cu 0.321%, S 0.024% and rest Fe was balanced, while in second samples the composition were C 3.81%, Si 2.64%, Mn 0.290 %, P 0.037%,Cu 0.325% and rest were balance. Austempering heat treatment process was done by first austenitizing the ductile iron by heating to 900 °C in an induction furnace and holding the temperature at that level for 1 h. Then, the samples were quenched in a salt bath at different temperatures. Two different techniques were used for the austempering process named single-step and two-step. In single-step austempering process, the samples were quenched from 900 °C in a salt bath having temperatures of 270, 300, 330, and 360 °C. The temperature of the salt bath was kept constant for 1.5 h. In two-step austempering process, the samples were quenched from 900 °C in the salt bath having initial temperatures of 260, 290, 320, and 350 °C. The salt was then heated just after quenching to final temperatures of 302, 332, 362, and 392 °C. The microstructure of all investigated austempered samples have shown graphite nodules dispersed in a matrix that consists of ferrite and carbon enriched austenite grains. Austenite grains appear as the bright phase while ferrite grains appear as the dark phase and graphite appears as black islands ‘‘nodules’’ dispersed within the matrix. For single-step austempered samples, the microstructure has changed from lower to upper ausferrite as the austempering temperature increased, On the other hand, in two-step austempered samples have shown a mixture of lower and upper ausferrite especially at lower levels of austempering temperatures.

A. S.M.A. Haseeb et.al.[35], compared the tribological behavior of quenched, tempered and austempered ductile iron at the same hardness level (445KHN). The chemical composition of ductile iron was 3.6%C, 2.5% Si, 0.6% Mn, 0.01% S and 0.02% P and balance Fe. For the heat treatment all the samples were austenitize at 860°C then quenching was done in brine and

tempered at 350°C.For austempering austentizes samples were transferred quickly to a lead bath maintained at 350°C. The samples were kept in the lead bath for 2 min, after which they were allowed to cool in still air for attaining the same hardness level. They found that wear rate increases with the increase of sliding distance. The rate of increase ishigher during the initial (running-in) period. After a sliding distance of $2*10^3$ m the wear rate attains a steady state value. The wear rate of austempered ductile iron is always lower than that of the quenched and tempered ductile iron. The rate of increase of wear rate as a function of load is much higher in the case of quenched and tempered samples than in austempered samples. Comparison of two samples show that the wear resistance of austempered iron is better than that of quenched and tempered iron at longer sliding distances. The morphology of the wear scars on quenched and tempered, and austempered ductile iron shows that in both cases scars show a similar morphology. These sliding marks running more or less parallel to each other are seen on the micrographs. The dark patches are thought to represent oxidized surface. The quenched and tempered samples show a decreased hardness below the worn surface while an increase in hardness is observed in the case of austempered samples. The difference between the wear resistance of quenched and tempered, and austempered ductile irons both having the same initial hardness can be related to the difference in their microstructures. Metallography and XRD reveal that the microstructure of quenched and tempered iron consists mainly of tempered martensite. XRD has revealed that austempered ductile iron used in the present study contains 23% retained austenite. However, the XRD pattern of the worn surface recorded after the wear test does not show any retained austenite peaks, indicating that during the wear process, retained austenite has been transformed and this transformation was martenstic transformation. So,under an applied stress resulting in an increase of hardness.

Jaun Manuel Velez et. al.[36], in this work have studied the abrasion resistance of ductile cast iron with different matrix microstructures (ferrite, pearlite, bainite and martensite) under high cantact stresses and strain rates. The composition of material used in this study was 3.5% C, 2.75% Si, 0.15% Mn, 0.038% P, 0.022% S, 0.005% Cu, 0.01% Ni and rest was balance Fe. Optical microscopy was used to analyse the microstructures. X-Ray diffraction was used to determine the volume fraction of retained austenite. The abrasion resistance experiment was

conducted in a modified charpy pendulum. The specimenwere held on a micrometric position table. The system was equipped with strain gauges to measure the tangential an d normal loads developed during the contact between the and the scratchier. The maximum scratch depth varied varied between 30 and 150 mm. corresponding the weight loss between 1 and 12 mg. As the depth of scratch increased, the difference between abrasion wear resistance for different microstructures and hardness become less pronounced. Micro cutting was main mechanism responsible for material removal in scratch test.

M.A**.** Shaker [37], studies the effect of graphite shape and nodularization percentage on the workability limits of various types of cast irons and secondly to study the effect of hardening- and tempering-treatment on the workability limits for the same various types of cast irons. Samples of gray, compacted and ductile cast irons were prepared from the same melt, having the chemical composition as 3.6 C, 2.4 Si, 0.54 Mn, 0.11 P, 0.05 S, rest balance Fe. The compacted graphite iron (80% nodularization) specimens were austenitized at 900 °C for 30 minutes in an electric resistance tube furnace with a controlled atmosphere to prevent surface decarburization or oxidation. After thatm the specimens were quenched immediately in cold water, so that their structure became martensitic. The specimens were then heated at different temperatures (400, 370, 350, 320 and 300 ° C) for 30 minutes and then cooled in air to determine the (optimum) tempering temperature which would result in the highest ductility. Other cast iron specimens were tempered at 350 °C for 30 minutes. Compression tests were carried out before and after tempering cast iron specimens having different nodularization percentages. The workability limits for the different types of cast irons were obtained and they found that a higher workability-limit is obtained for spheroidal graphite irons, the workability-limit reducing as the nodularization percentage decreases: the lowest workabilitylimit is obtained when the nodularization percentage is zero (flaky-graphite cast iron).So the nodularization percentage, the shape, the size and the distribution of the graphite particles are the controlling parameters of the overall mechanical properties, the fracture behaviour and the workability limits of the cast irons. The graphite nodules can be considered as voids in the material, surrounded by the matrix. The role of the graphite particles is to decrease the cross-sectional area supporting the applied load. In addition, because a void represents a local stress-concentration, the average maximum normal stress on the specimen is increased significantly throughout the specimen, providing a

detrimental effect. The development of microcracks around the cavities (graphite particles) depends on the cavity shape and the radius of curvature of the graphite particle is also a major parameter on which the maximum stress level depends. The stress concentration factor ranges between 3 for spheroidal-graphite particles to 30 for flaky-graphite particles. The variations of compressive strength with tempering temperatures were also studied and found that the compressive strength minimum at 350 °C tempering temperature, while maximum at 400 ° C tempering temperature. The greatest ductility of the cast ions treated was obtained at 350 °C tempering temperature. The workability-limit of the compacted graphite cast iron being intermediate between that of the flaky-graphite cast iron and that of the spheroidal-graphite cast iron. Thus, they conclude that the hardening and tempering treatment increases the workability-limits for the cast irons.

C. D'Amato, C. Verdu et.al. [38], Characterize the austempered ductile iron through Barkhausen Noise Measurements (MBN) as a nondestructive method for characterizing the microstructure of ADI. The chemical composition of three different samples used in this work was C 3.6%, Si 2.4%,Mn 0.2%, S and P 0.02%, Mg 0.04%, Cu 0.02% and in other two samples other elements were same except Cu (0.8%), Mo(0 and 0.2%) and Ni (0.5%). These samples were firstly fully austenitized in the temperature range 850°C–950°C. Then they were rapidly cooled to the temperature range suitable for bainite reaction. Austempering consists of an isothermal holding in the temperature range 250°C–450°C for 0.5–2 h before cooling to room temperature. During austempering, bainitic ferrite nucleates and grows into the austenite. The high silicon content (<2%) of ductile irons hinders the precipitation of carbides during the transformation. Carbon diffuses from the supersaturated ferrite into the surrounding austenite and the nontransformed austenite is gradually stabilized, allowing it to be finally retained when the material is cooled to room temperature. The period between the end of stage I and the beginning of stage II is referred to as the "process window"and corresponds to highest retained austenite contents and the best mechanical properties.To obtain a wider process window, alloying elements, such as Mo, Ni, Mn, or Cu, which delay the both stages of the bainite reaction, are added. Two types of ADI are usually distinguished which are at temperatures below 330°C ferrite units look like fine needles or laths and the microstructure is called "lower bainite" and

other is at temperatures above 330°C , the microstructure consists of coarser ferrite plates arranged in sheaves and is referred to as “upper bainite.” Microstructural characterization has been performed by Optical and scanning electron microscopy observations after polishing and etching with 4% Nital. The expected microstructures have been obtained for the constituents of the SGCI samples after particular treatment. For the series of ADI samples, the evolution of the bainitic matrix with the heat treatment parameters also has been studied in which scanning electron micrographies show that the bainitic microstructure becomes coarser with increasing austempering temperature. X-ray diffraction measurements with Co targetwas used to quantify the progress of the bainite reaction. Retained austenite volume fraction is calculated using the ratio between several diffraction peaks of ferrite (200, 211, 220) and austenite (200, 220, 311, 222). The volume fraction of retained austenite never significantly increases with increasing austempering time and a drop of the retained austenite volume fraction is observed for samples austempered at 425°C for long time, which indicates that the II stage of the bainite reaction had been reached. Magnetic Barkhausen Noise was measured by using a magnetic circuit, a U-shaped core made of a high permeability iron-nickel alloy closed through the cylindrical sample was magnetizd by means of a coil wound around the U-shaped core. The magnetic field H induced in the samples is measured at its surface by a Hall sensor. The samples are magnetized from saturation to saturation with a quasi-triangular waveform. The electromagnetic signals are detected using a surrounding coil probe. SGCI with ferrite or pearlite exhibits a very high peak at low magnetic field(HM 0.2 and 1 kA/m) while SGCI with martensite or bainite exhibits a much smaller peak, whose amplitude is about 10 times or so smaller than that of SGCI with ferrite or pearlite. In addition, these peaks appear at higher fields (HM ranging from 2 to 3.6 kA/m).

O. Eric, L. Sidjanin et. al.[39], studied the effect of austempering on the microstructure and toughness of nodular cast iron alloyed with molybdenum, copper, nickel, and manganese. The Chemical composition of CuNiMo SG ductile iron were divided in three groups as Light microscopy , scanning electron microscopy , and X-ray diffraction technique were performed for microstructural characterization, whereas impact energy test was applied for toughness measurement. Specimens were austenitised at 860 °C, then austempered for various times at 320

and 400 °C, followed by ice-water quenching. The microstructure analysis shows that in as-cast specimens the graphite nodules in CuNiMo SG ductile iron were not uniform in size and distribution. After austenitising at 860 °C and austempering at 320 °C for 1 h, some amount of martensite was observed in the microstructure.The microstructure of the specimen austempered at 320 °C for 2.5 h exhibits a typical lower bainite structure with an acicular appearance of bainitic ferrite and retained austenite. Prolonged austempering time of 5 h was distinguished by the feathery bainitic ferrite. Only martensitic structure appears throughout the whole austempering interval at 400 °C. X-ray diffraction pattern of specimen's austempered at 320 and400 °C for different times shows the Fe3C-type carbides are formed after 0.5 h of austempering. While isothermal transformation at 320 °C in the time interval from 2 to 5 h produced bainitic ferrite containing transitional ε-(Fe2C) carbides with the hcp crystal structure was formed. The formation of ε-carbides in bainitic ferrite together with the high-volume fraction of retained austenite might be the result of the progression of the stage I reaction. These carbides that appear on the ferrite/ austenite interface are the products of the decomposition of the high-carbon retained austenite according to the stage II reaction. After 3 h of austempering at 400 °C, Fe3C is still present in the microstructure together with ε-carbides. Fractographs were also taken by using SEM from the surface of fractured specimens austempered at 320 and 400 °C from 1 to 5hrs. Austempering at 320 °C for 2 hrs produced a ductile fracture, in which manysmall voids, were associated with ε-carbides. The fracture surface consists of widely spaced large dimples, which are related to the graphite nodules, separated by regions containing arrays of fine dimples. On austempering at 320 °C for 3 h the mechanism of fracture is mixed (consisting of ductile and quasi cleavage modes) mode. After 5h of austempering the fracture mode was mostly brittle and described as the higher concentration of precipitated ε-carbides. On the other side, the brittle fracture of all specimens austempered at 400 °C was a consequence of both the martensitic structure and the presence of m-carbides on the ferrite/austenite interface boundaries. The highest-impact energy corresponds to ductile fracture that prevails as a fracture mode. With longer time of austempering toughness decreases to the level between 85 and 90 kJ. On the contrary,specimens austempered at 400 °C possess very low values of impact energy (between 10 and 12 kJ) from 0.5 to 5 h of austempering. Such a behaviour was related to the microstructure in which martensite predominantly appears, and provokes the brittle fracture through the whole austempering interval.

A.R. Kiani-Rashid[40], studied the influence of austenitising conditions and aluminium content on microstructure and properties of ductile iron. The microstructure analysis shows that pearlitic matrix is obtained in the as-cast irons before further isothermal heat treatments. It was believed that the nucleation of austenite in ferrite/cementite boundaries is easier than at the ferrite/graphite interface and diffusional distances were decreased by a finer pearlitic matrix and aluminium addition improves the pearlite formation in ductile irons. Hardness increases with increasing austenitising time, due to transformation of the initial microstructure of austenite to martensite. An incomplete austenitising reaction at shorter times results in a lower hardness. However, with extended austenitising time, the hardness shows a decrease due to the larger size of austenite grains. So this time will be optimum. Thus, they found that austenitising was able to reduce the inhomogeneity of as-cast microstructure and the segregation profile of Al and Si decreased markedly with incrsasing austenitising time for different levels of aluminium.

Megnus Wessen et.al.[41], studied the growth of ferrite in noduler cast iron by thermal analysis of cooling in plate casting as well as by quenching of remelted samples in a furnace having a constant cooling rate. They took the plates with the thickness 4, 8, 15, 30, 50 mm. have been cast in a furnace bonded quartz sand. The composition of sample was C 3.73%, Si 2.6%, Mn 0.23%, P 0.02%, S 0.007%, Mg 0.0445, Cu 0.041% (all in wt %). The temperature and time data's were recorded by two thermocouples, one for the control of the furnace and other positioned in the center of the sample. The heating rate was 10K/ min. Heating were interrupted when the furnace temperature reached 1220°C. The temperature kept constant until the temperature of the sample held reached 1100°C, ensuring the sample was melted and providing time for graphite dissolution. Quenching was done in 10% NaCl water solution. In each sample the nodule count, the ferrite and pearlite fraction, the thickness of the ferrite shell and hardness were measured. They noted that the reaction starts at approximately at the same time for all plates, but the maximum transformation temperature decreases with plate thickness. The total time for transformation was also noted. They found that the ferrite/ pearlite interface coefficient depend on the nodule size i.e., decreases with the decrease in nodule size. They concluded that

the growth of ferrite can be divided in three different stages i.e. diffusion of carbon away from the austenite/ferrite interface into austenite, incorporation rate of carbon atoms on to the graphite surface and the diffusion of carbon through the ferrite shell.

M. Heydarzadeh Sohi, M. Nili Ahmadabadi and A. Bahrami Vahdat[42], investigated the role of austempering parameters on the structure and the mechanical properties of ductile iron. The chemical composition of the sample was: 3.5% C, 2.5% Si, 1.1% Ni, 0.6% Cu, 0.23% Mo and 0.3% Mn. Tensile specimens together with the samples for hardness and microstructural testing were machined. These specimens were austenized at 900°C for 2 hours and then austempered at 315°C and 350°C for 30, 60, 120, 180, 240 and 360 minutes. Tensile, impact and hardness testing were done according to ASTM-E8, ASTM-A897 and DIN5O351 standards, respectively. The morphology of bainite in the samples which were austempered at 315°C was acicular whereas in the samples which were austempered at 350°C, it seemed to be transitional bainite. The amount of martensite in the austempered samples decreases by increasing austempering time. Austempering at 350°C resulted in higher ductility,lower strength and hardness values compared to austempering at 315°C. In both the samples which were austempered at 315°C and 350°C, respectively, the tensile strength, yield strength, % elongation increases with austempering upto a certain critical value of austempering time and then decreases. Highest hardness was observed in the sample which was austempered at 315°C for the shortest time. The optimum structure and mechanical properties after austempering at 350°C and 315°C were obtained in 180 and 240 minutes, respectively.

Weimin Zhao and Guixin Wang[43], carried out experiments to control the microstructure and mechanical properties of ductile for it’s as liner plates. The experiments showed that lowering the austenizing and austempering temperature can produce a large bainite content faster, which means the the production speed increases. It was found that an austenite content of 3-9%, a bainite content of 60-85% and a martensite content of 10-23% is suitable for liner plates of a grinding mill. The wear life of such liner plates was found to be three times more than the liner plates made of high manganese steel. The hardness increases with the increase in the

amount of lower bainite. The experimental results showed that reducing the austenizing and austempering temperatures can speed up the formation of bainite. Thus, it was concluded that bainite liner plates can overcome the disadvantages of high manganese steel.

Karl-Fredrik Nilsson, Darina Blagoeva and Pietro Moretto[44], studied and correlated the variation inductility with dects and microstructure of ductile cast iron. This paper describes a statistical test plan to determine tensile properties and fracture properties of ductile cast iron considered for the Swedish nuclear waste canisters. A large number of tested tensile specimens were subsequently analyzed by fractography and metallography to relate the low ductility values to size and type of casting defects. Loss of ductility can be due to high pearlite content, low nodularity, slag defects and chunky graphite. Slag defects were modeled by an elasto-plastic fracture mechanics model for penny-shaped slag defects and semi-empirical models for other types of defects. The computed ductility distribution agreedvery well with measured data whereas the computed defect size distribution was under-estimated. By including crack growth resistance and various aspect ratios of defects, a much better agreement with observed defects can be achieved.

J.P. Monchoux, C. Verdu and R. Fougeres[45], investigated the effect of ferritization heat treatment on the fracture toughness of ferritic S.G. Cast iron. Because of the high ductility of the material, $J_{0.2/BL}$ values were measured instead of K_{IC} values. The crack length was indirectly measured by compliance variations induced by the reduction of the loaded area due to the crack growth. It was found that $J_{0.2/BL}$ values increased by ferritization heat treatment. This was explained by the disappearance of the pearlitic brittle phase. The weakening of the matrix-graphite interface after the heat treatment remains small and cannot compensate the former effect. The $J_{0.2/BL}$ values measured were found approximately constant with the Silicon content for the investigated materials.

J.H. Zhu, P.K. Liaw, I.M. Corum, J.C.R. Hansen and J.A. C'ornie[46], have studied the damage mechanisms in ductile cast iron. The chemical composition of the material investigated was: 3.4-3.8% C, 2.0-2.7% Si, 0.3-0.6% Mn, 0.08% P, 0-2.5% Ni and remaining Fe. For microstructure observations, the samples were mechanically polished and etched in a 2% Nital solution. The microstructures and fracture surfaces, both were observed under optical microscope and SEM. The optical microstructure revealed a "bull's eye" structure of graphite nodules (average diameter = 25μm) surrounded by ferrite in a matrix of primary pearlite. The average graphite nodule content was 10 volume %. The fracture surface for the single-edged notched beam specimen showed that the crack initiates at the interface between the graphite and surrounding ferrite. The crack propagates following the graphite nodule enriched path. The cracks get arrested by the ductile ferrite that surrounds the graphite nodule, thus absorbing energy and leading to high fracture toughness values. The fracture surface had three distinct features:

- Graphite particles (which debonded from the surrounding ferrite).
- Cleavage regions (which resulted from the failure of pearlite).
- Ductile dimples (primarily surrounding the graphite particles).

Thus, the ferrite surrounding the graphite nodules is the main contributor to fracture resistance of ductile iron, since it arrest the cracks by absorbing the energy.

F.T. Shiao, T.S. Lui, I.H. Chen and S.F. Chen[47], have studied the cell wall morphology and tensile embrittlement in spheroidal ferritic graphit cast iron. Four S.G. cast iron samples having varying chemical compositions and carbon equivalents were chosen in this study. They were designated as A3.9 (3.42% C & 3.89% Si), A2.7 (3.47% C &2.68% Si), A2.0 (3.54% C & 2.02% Si) and B2.1 (1.95% C & 2.11% Si). The as-cast S.G. cast irons were heat treated to fully pearlitic matrix. During heat treatment, the specimens were first held at 920°C for 3 hours, then furnace cooled to 730°C where it is held for % hours and finally it was furnace cooled to room temperature. The tensile specimens of 6mm diameter and 30mm gauge length were sectioned from the direction perpendicular to the casting riser. The tensile tests were performed. The testing temperature were varied from 30-520°C for A3.9, -120°C to 520°C for A2.7, -120°C to

85°C for A2.0 and -120°C to25°C for B2.1. Each specimen were held isothermally at it's chosen temperature before conducting the test. The temperature fluctuations were within ±2°C during the entire testing period. To reveal the morphology and distribution of the eutectic cell walls, the test materials and selected deformed tensile specimens were electrochemically etched in Morries solution. Morries solution was prepared by mixing 7cc of H_2O, 133cc glacial acetic acid and 25gm CrO_2. The electrochemical etching process uses a 304 stainless steel as the cathode and need an applied voltage of 5V. The total etching time for all the cases was 30 minutes. In order to provide quantative data for further analysis, the average area and average length of the eutectic cells of each test materials were measured. The length of the cell wall was measured along the longest axis. From SEM analysis, it was found that the eutectic cell wall size decreases with decreasing Silicon content. The yield stress also decreased with the increase in testing temperature. Also, the yield stress was found to be higher in the sample with higher Si content and lower C content. From optical microstructure analysis, It was found that the graphite nodule size of A2.7 was 40.4µm and slightly smaller than the size of 50±2µm for the other three. Micrographic features showed that the average size of the eutectic cell walls and thus the amount of inclusion particles clustered in the cell wall regions decreases with decreasing Si concentration. The fractured surface showed zoned ductile fracture and zoned brittle fracture (in the intermediate low temperature range) when tested at the tensile temperatures around -30°C. A large eutectic cell wall size with a larger amount of inclusions in the cell walls give rise to elongation deterioration at temperatures around 400°C. It was shown that the inclusions clustered in the eutectic cell wall regions are the main culprit for the generation of intergranular fractures.

Kong Zhou, Yehua Jiang, Dchong Lu, Rongfeng Zhou and zhenhua Li[48], have developed a wear resistant bainite/martensite ductile iron which is characterized by a combination of alloying elements and controlled cooling. The chemical composition of the ductile iron used in this work was (in Wt %) 3.2% C, 2.5% Si, 2.5% Mn, 0.06% S, 0.06% P and remaining iron. The sample was a round bar of 3mm in diameter and 10mm in length with ahole of 2mm diameter and 2mm length in it to weld a thermocouple. The austenization temperature was 900°C. The holding time was 5 minutes. The heat treatment process was carried out in such a manner that we obtain a bainite-martensite dual-phase structure. The samples were heat treated

by the controlled cooling process. At the end, tempering at 250°C for 2 hours was done to remove the residual thermal stresses in the samples. The controlled cooling heat treatment process consisted of three stages. In the first stage, water spraying was done to quench the samples from the austenization temperature to 300°C in a few minutes. This allows the samples to avoid pearlitic transformation. In the second stage, the samples were held at 200-300°C for 2 hours so that bainitic transformation takes place.This stage is also called heat preservation stage. Finally, the samples were taken out from the heat preservation setting and air cooled to room temperature for martensite formation. The wear sample was a cylinder with a diameter of 10mm. The impact wear tests were carried out using a MLP-10 impact abrasive wear tester. The wear surfaces were 50mm arc surfaces. The feed velocity of the abrasive was 50 Kg/hr. The impact energy was 2 Joule. The wear characteristic of the material was characterized by weight loss method. The phase analysis was performed on a Siemens U500 X-ray diffraction auto analyzer.

CHAPTER 3

Experimental Procedure

CHAPTER3

3 Introductions:

This chapter introduces the experimental procedure utilized to characterize the ductile iron studies.

3.1 Raw Materials

Ductile iron produced in a commercial foundry known as L&T kansbahal, has been used for this experiments. Two grades of ductile iron were used. The differences between these two grades were: one contains copper, while other was without copper. They were designated as Grade A and Grade B. Chemical compositions of raw material obtained by weight chemical analysis method used in this study are given in Table 3.1.

Table 3.1

All are in wt %	C	Si	Mn	Cr	Ni	Mg	Cu	S	P
Grade A	3.55	2.1	0.18	0.03	0.12	0.038	0.41	0.009	0.024
Grade B	3.57	2.22	0.23	0.03	0.42	0.045	……	0.011	0.026

3.2 Test Specimen Preparation:

For different tests the solid block of ductile iron was cut to thickness of 4-6 mm using power hacksaw. Then they are grinded, polished and machined to the dimension required for various experiments to be carried out.

3.3Heat Treatment:

Twenty samples from each grade were taken in a group. To homogenize the samples kept them in a muffle furnace for one hour at 927°C, some samples were conventionally treated and some were austempered for different times with constant temperature.

3.3.1Annealing and Normalizing:

After austenization for annealing samples were cooled in furnace for 12hrs and normalizing was done by rapid cooling of samples in still air for 30 minutes.

3.3.2: Quenching and Tempering:

After austenization some samples were quenched in oil for 20 mins. Apart from two or three samples rest were tempered at 200°C, 400°C and 600°C for 1 hrs.

3.3.3 Austempering:

For austempering, the samples were heated at 925°C for 1 h for austenization and then transferred quickly to a salt bath (salt combination was 50 wt % $NaNO_3$ and 50 wt % KNO_3) maintained at 260°C. The samples were kept in the salt bath for different times as 30 mins, 1 hr, 1.5 hr, 2 hr. After which they were allowed to cool in still air. The isothermal austempering cycle used in this study is shown in figure 3.1.below.

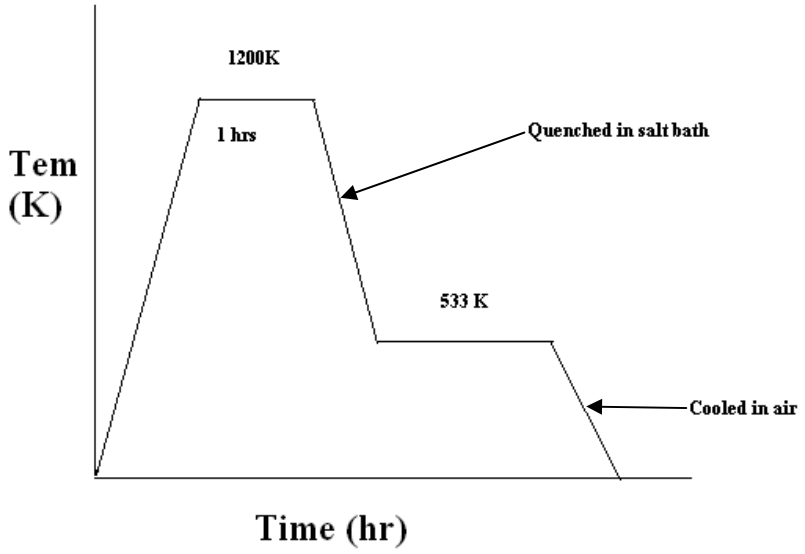

Fig 3.1: Isothermal cycle for austempering treatment.

3.4 Hardness Measurement:

The heat treated samples of dimension 8×8×3 mm were polished in emery papers(or SiC papers) of different grades for hardness measurement. Rockwell Hardness test was performed at room temperature to measure the macro hardness of the ductile iron specimens in A scale. The load was applied through the square shaped diamond indenter for few seconds during testing of all the treated and untreated samples. Four measurements for each sample were taken covering the whole surface of the specimen and averaged to get final hardness results. A load of 60 kg was applied to the specimen for 30 seconds. Then the depth of indentation was automatically recorded on a dial gauge in terms of arbitrary hardness numbers. Then these values were converted to in terms of required hardness numbers (as Brielle's or Vickers hardness numbers).

3.5 Tensile Testing:

. Tensile test were carried out according to ASTM (A 370-2002). Specimens of "Dog Bone Shape" shown in figure 3.2 were prepared for tensile test, which were machined to 5mm gauge diameter and 30 mm gauge length. Test were conducted by using Instron 1195 universal testing machine connected to computer to draw the stress–strain curves and recording the tensile strength, 0.2 proof stress and elongation. Test were performed at room temperature (298K) with strain rate of 9×10^{-3} up to fracture. The tensileload of 50 KN was applied to the specimen up to the breaking point.

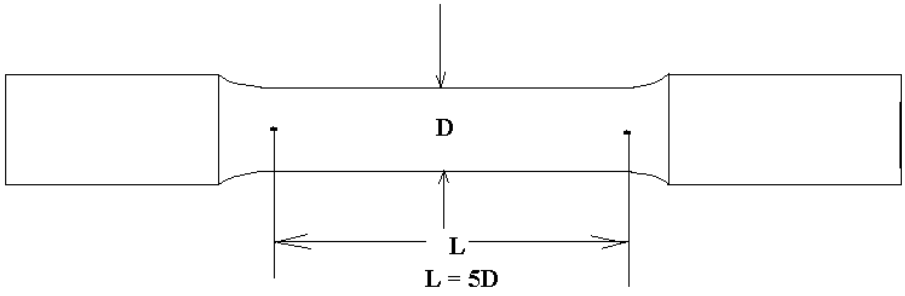

Fig 3.2: Specimen used for tensile properties

Advanced materials are used in a wide variety of enviournments and at different temperature and pressure. It is necessary to know the elastic and plastic behavior of these

materials under such conditions. Such properties as tensile strength, creep strength, fatigue strength, fracture strength, fracture toughness, and hardness characterize that behavior. These properties can be measured by mechanical tests. The picture of tensile testing machine used in our laboratory is Instron 1195, which is given in fig 3.3.

Fig3.3: Instron 1195

3.6 Optical Investigation:

3.6.1 Micro-structural observations:

Before and after heat treatment, the samples were prepared for micro structural analysis. From each specimen a slice of 4 mm is cut to determine the microstructure. These slices are firstly mounted by using Bakelite powder then polished in SiC paper of different grades (or emery papers) then in 1 µm cloth coated with diamond paste. The samples were etched using 2% nital (2% conc. Nitric acid in methanol solution). Then the microstructures were taken for different heat treated specimen by using Scanning Electron Microscopy (SEM).

3.6.2 Fractoraography:

Fracture surface or surface morphology of the samples which fractures in different manners (ductile, Brittle and mixed mode fracture) after tensile test for treated and untreated condition are analyzed by using Scanning Electron microscopy (SEM).For this samples were cleaned with Acetone to remove any dust or impurity on the surface of specimens before SEM.

3.7 X-Ray Diffraction studies:

The X-Ray diffraction (XRD) analysis was performed for few selected samples. This technique was used to estimate the volume fractions of retained austenite, ferrite, martensite, in the material after treatment. XRD was performed 30 KV and 20 mA using a Cu- Kα target diffractometer. Scanning was done in angular range 2θ from 40° to 48° and 70° to 92° at a scanning speed of 1°/min. The profile were analyzed on computer by using X' Pert High Score Software to obtain the peak position and integrated intensities of the {2 1 1}.{110} plane of BCC ferrite and {111},{220},{311}planes of FCC austenite. By comparing these intensities the volume fractions of retained austenite and ferrite were estimated.

CHAPTER 4

Result and Discussion

CHAPTER 4

4.1 Mechanical Properties:

The mechanical properties measured by using Instron1195and dimensions of specimen was carried out according to ASTM (A 370-2002), are given in Table 4.1 (a),(b) and 4.2(a),(b) lists the mechanical properties viz. Tensile strength, 0.2% Proof stress, % Elongation, Hardness etc. of cast irons (with and without Cu addition) respectively.

Treatment	U.T.S (MPa)	0.2% Y.S.(MPa)	% Elongation	Hardness(RA)
Annealed	371.3	185.6	19.05	49
Normalized	408	158	7.28	60
Oil quench	419	172.9	4.48	79
Temp 21	399	217.1	8.1	71
Temp 41	340	205	12.02	67
Temp61	310.5	194	14.7	65

Table 4.1(a): Mechanical properties of treated ductile iron with Copper

Treatment	U.T.S(MPa)	0.2% Y.S(MPa)	% Elongation	Hardness(RA)
Annealed	242.7	205.3	18.10	45
Normalized	464	219	8.85	72
Oil quench	350	240	5.02	78
Tem21	320	210	9.17	70
Tem41	280	194	13.34	62

Tem61	240	169	16.8	58

Table 4.1 (b): Mechanical properties of treated ductile iron without Copper

*U.T.S. - Ultimate Tensile Strength,

*Y.S. – Yield Strength

*Temp21,41,61-tempered at 200°C,400°C, 600°C for 1 hrs.

Treatment	U.T.S(MPa)	Y.S.(MPa)	% Elongation	Hardness(RA)
Austempered 0.5	872.5	154	21	72
Austempered 1.0	967	170	13.51	71
Austempered 1.5	745	163.9	17.45	66
Austempered 2.0	715	147.7	10.05	62

Table 4.2 (a): Mechanical Properties of austempered ductile iron with Copper.

*The subscript in austempered denotes the time of austempering.

Treatment	U.T.S(MPa)	Y.S.(MPa)	% Elongation	Hardness(RA)
Austempered 0.5	850	175	33	71
Austempered 1.0	942	190	15	60
Austempered 1.5	730	195	22	64
Austempered 2.0	685	138	19	60

Table 4.2 (b): Mechanical Properties of austempered ductile iron without Copper.

4.1.1 Hardness measurement:

. Figure 4.1.1 (a) and (b) shows the variation of hardness values in (Rockwell Hardness 'A' scale) with the treatment conditions. The Fig. 4.1(a) shows that hardness decreases as the tempering temperature increases in both cases (with Cu and without Cu additions). This is due to the transformation of martensite to tempered martensite. The hardness of martensite is due to the tetragonal structure of the martensite where carbon occupies tetrahedral voids. This structure results from the diffusion less transformation which occurs by shear mechanism. So when martensite is tempered, diffusion of C from the tetrahedral sites of the BCT structure takes place and thus the tetragonality of martensite gets reduced. Alternatively, the structure of martensite becomes less strained after holding it at a higher temperature but less than the lower critical temperature because of carbon diffusion. Thus, the hardness of tempered martensite is lesser than quenched martensite.[17]

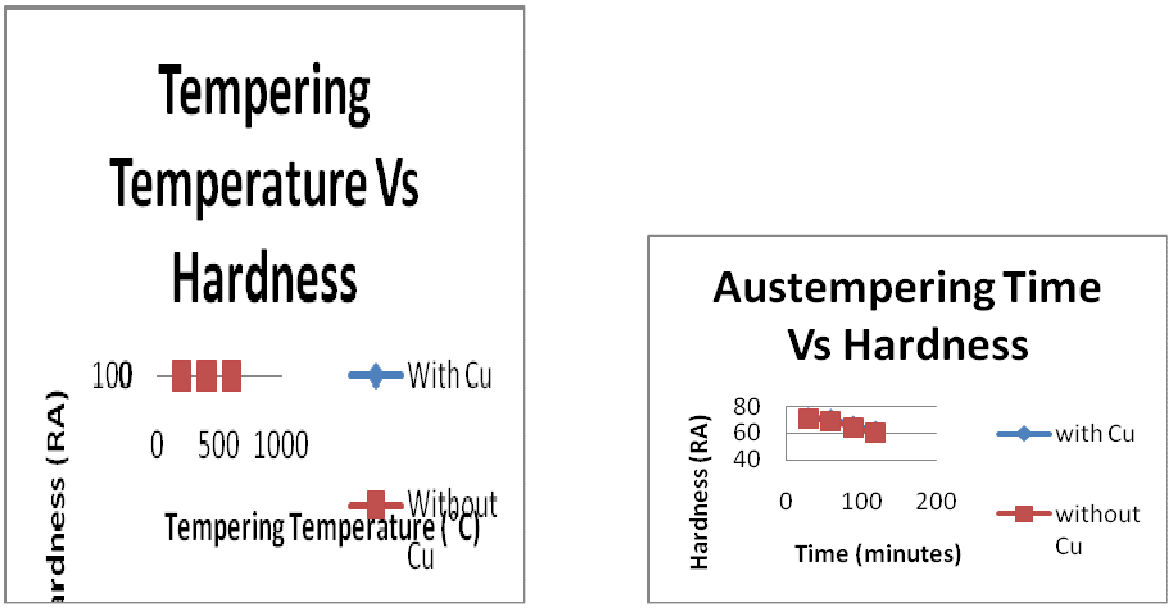

(a) (b)

Fig 4.1.1: Variation of hardness with tempering temperature and austempering time.

For austempered samples the variation of hardness is shown in figure 4.1 (b). Hardness of plain ADI is slightly lower than the Cu enriched ADI, and hardness reduces proportionally with increase in austempering time. This decrease in hardness is due to the disappearance of martensite phase. Lower austempering time yield a finer structure and therefore higher hardness was obtained. But as the holding/treatment time increased further, the hardness

values were again decreased due to the occurrence of coarse plate-type structure (of bainitic) matrix phase.[22,23]

4.1.2 Tensile Strength and Elongation:

The variation of U.T.S., 0.2 % proof stress and elongation with temperature in the case of tempering, and with time for austempered samples, of two different grades are shown in figure 4.1.2 (a), (b), (c) and (d),(e), (f).

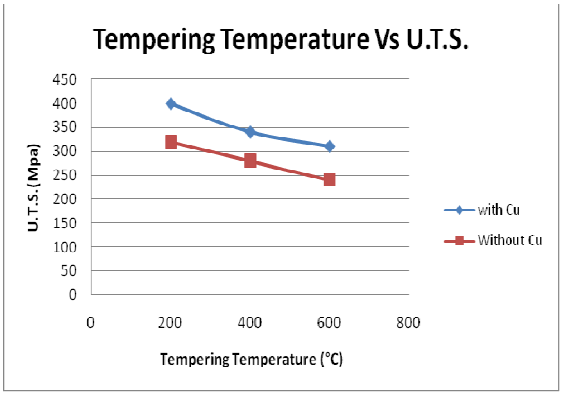

(a)

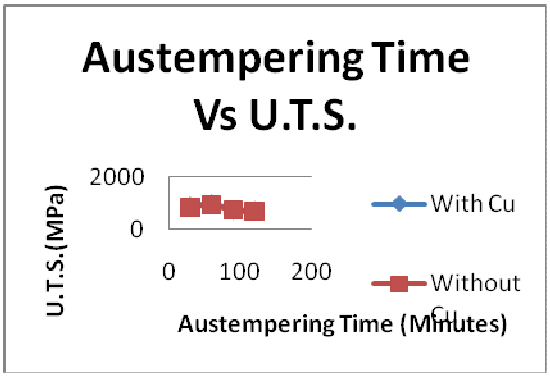

(b)

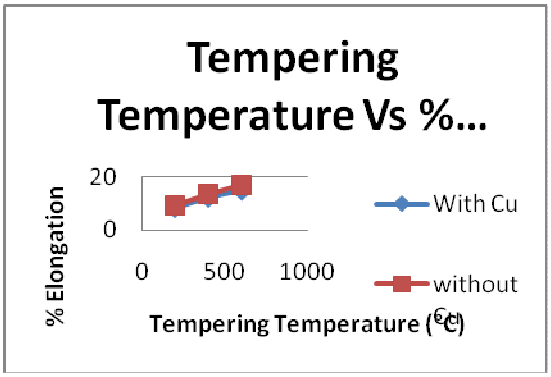

(c) (d)

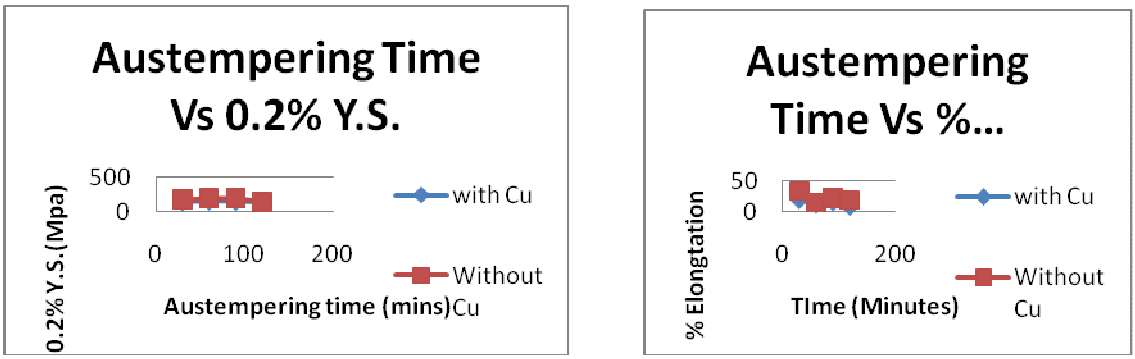

(e) (f)

Fig 4.1.2: Mechanical properties with different treatment conditions

Comparing the tensile strength of two different grades of samples with different treatments, it is observed that, there is a slight change in their properties. The U.T.S of normalized samples was greater than the annealed samples but less than the tempered and austempered samples. The tensile properties vary with the matrix type, i.e. - pearlitic (in case of normalized samples), martensitic (in case of quenching and tempering) and bainitic (in case of austempered samples) matrix. So 0.2% proof stress and U.T.S increases but elongation decreases depending on pearlite content of the matrix. Tempered samples have higher tensile properties than the normalized samples, but as the tempering temperature is increased there was a decrease in U.T.S and 0.2% Y.S, as shown in fig 4.1.1(a) and (b). The elongation of tempered samples is less than annealed sample but higher than narmalised samples, because of the formation of martensite and tempered martensite etc.. On the other hand, the ductility (% elongation) increases with the tempering temperature as shown in figure 4.1.2 (c).[17,25]

By austempering treatment, the variation of mechanical properties depends on the change in the nature and amount of transformation/formation of bainite phase. At lower austempering times, the U.T.S., 0.2% proof stress and elongation increases initially, then decreases and with further increase in treatment time attains a steady state, as shown in fig 4.1.2 (f). But with longer austempering times, the value of U.T.S., 0.2% proof stress decreases. The decrease in elongation while austempered for an intermediate time range may be due insufficient unreacted low carbon austenite. But as the time increases further, the retained austenite reduces, and ductility again

increases with time. The increase in strength initially at low time interval is due to the high amount of martensite derived from the unreacted austenite, but as the time increases above 30 minutes the first stage reaction commences in the intercellular regions for which strength decreases and ductility increases further to a maximum value; that indicates the tolerable amount of martensite. The sample alloyed with copper has increased ductility and lesser strength than that of the sample with out copper content.[22,28]

4.2 Optical investigations:

4.2.1 Microstructures:

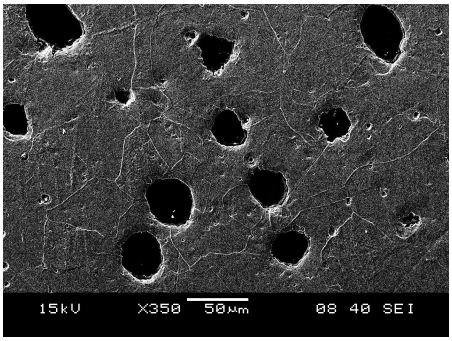

(a)Annealed (Gd A)

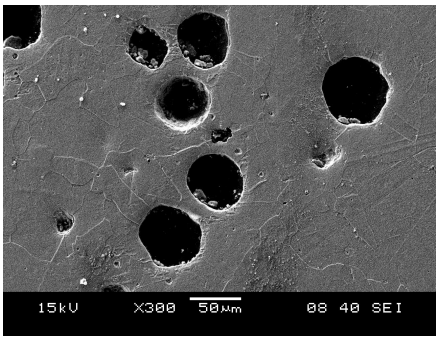

(c) Annealed (Gd B)

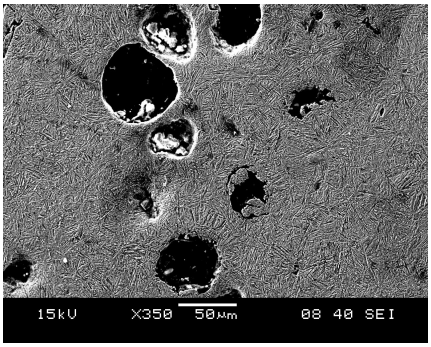

(d) Normalised (Gd A)

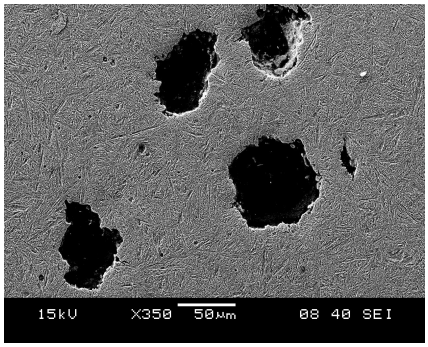

(e) Normalised (Gd B)

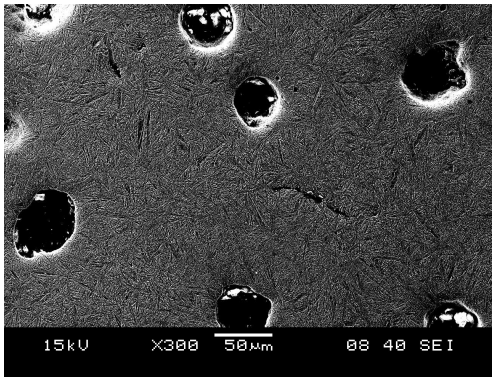

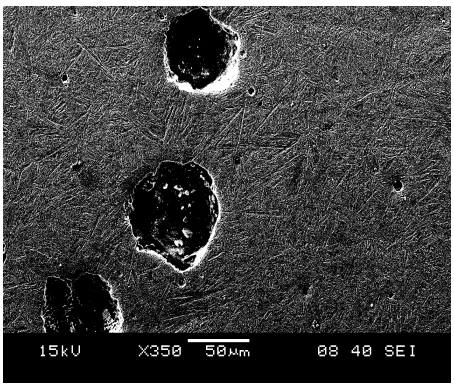

(e) Tempered2 (Gd A)

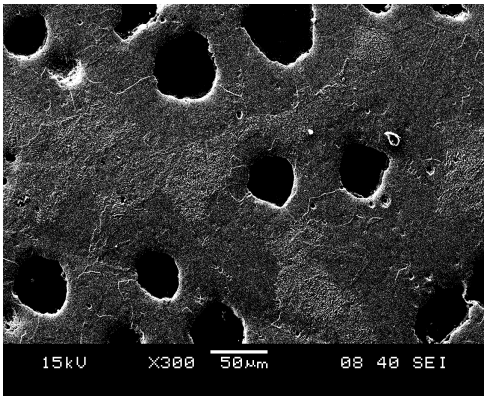

(f) Tempered2 (Gd B)

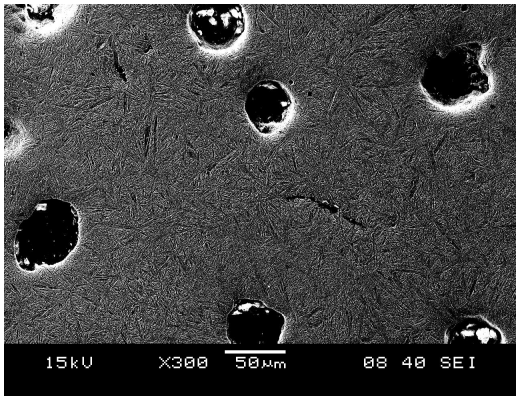

(g) Tempered 4(Gd A)

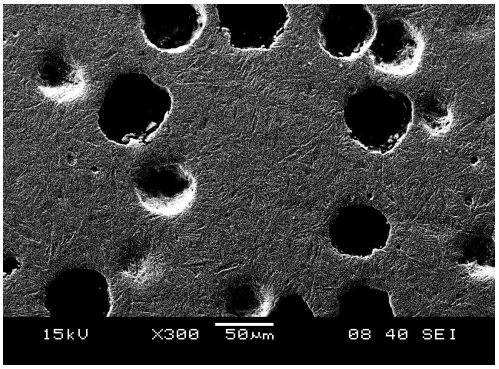

(h) Tempered 4 (Gd B)

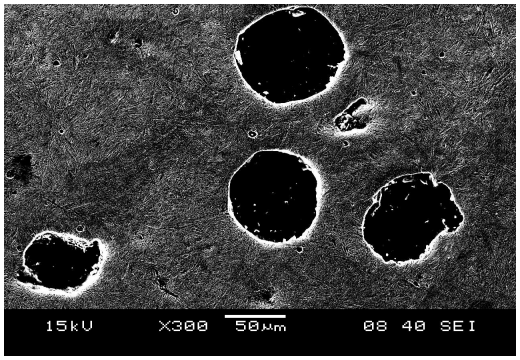

(i)Tempered 6 (Gd A)

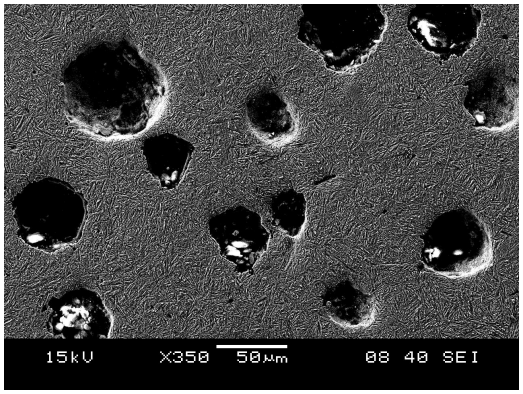

(k) Tempered6 (Gd B)

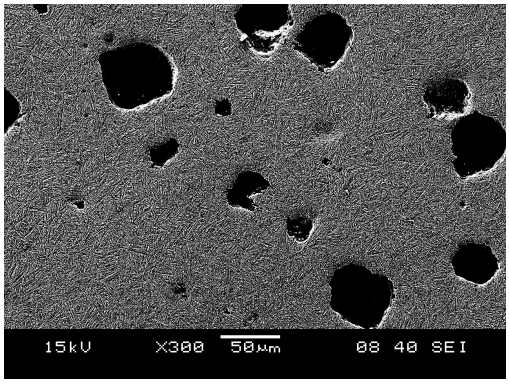

(k) Austempered0.5 (Gd A)

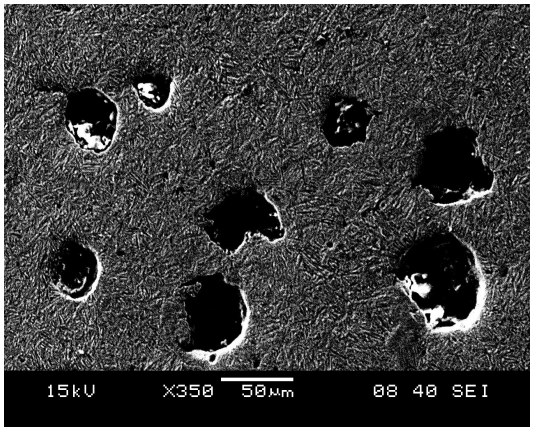

(l) Austempered0.5 (Gd B)

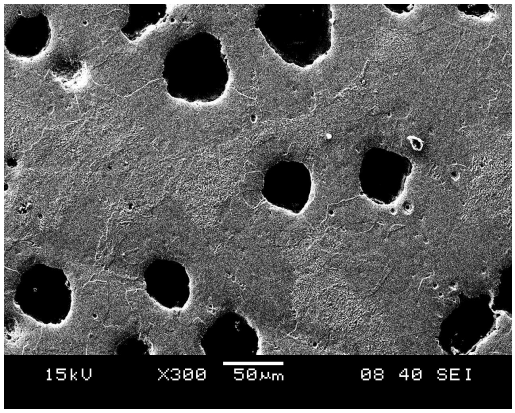

(m) Austempered 1(Gd A)

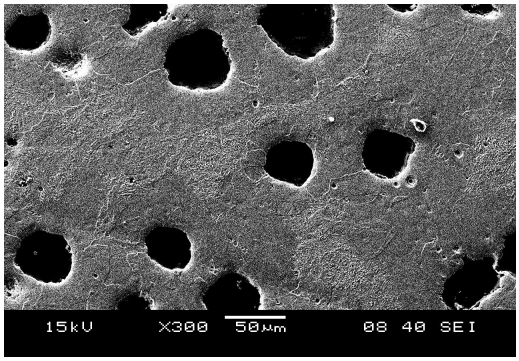

(n) Austempered 1(Gd B)

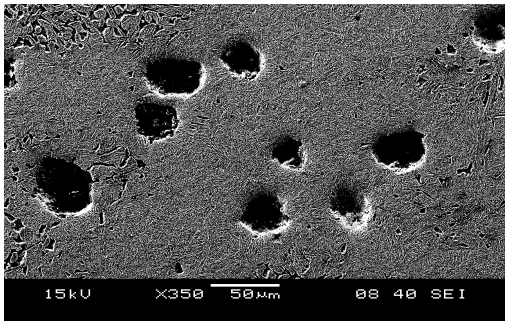

(o) Austempered 1.5(Gd A)

(p) Austempered 1.5 (Gd B)

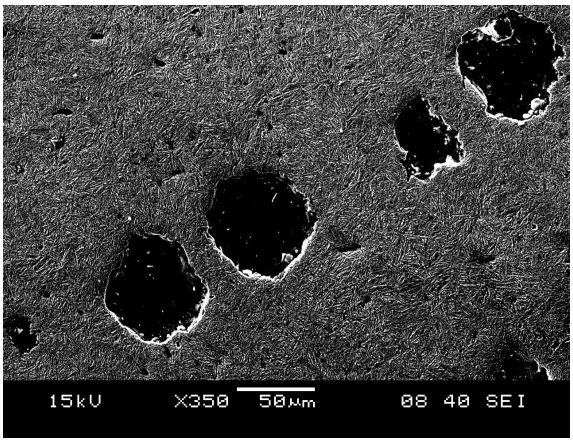

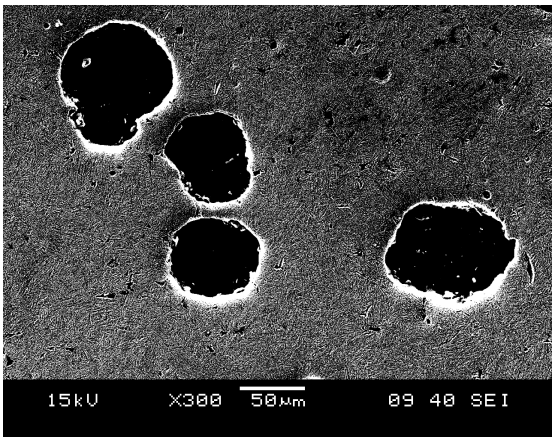

(q) Austempered 2 (Gd A)

(r) Austempered 2(Gd B)

Fig 4.2.1: Microstructures of differently heat treated samples for two different Grades**.**

*Gd A & Gd B represents: samples with Cu and samples without Cu.

*Temperd2, 4, 6 represents tempering at 200, 400, 600°C.

* Austempered 0.5, 1, 1.5, 2 represents the time of austempering in hours at constant temperature.

The microstructure of ductile iron in as cast condition is mostly pearlitic.[22] After different treatments there is a change in matrix/phase structure, number of nodules and their spheroidicity. These cause changes in the mechanical properties of ductile iron. The microstructures after different types of treatments of two different grades are shown in figur4.2.1 from (a) to (r).There is although not much differences in the matrix pattern of two different grades (with Cu and without Cu) of ductile iron, but the number of nodules and nodule count in case of grade A is higher than grade B. Also there is a change in the length /and sharpness of (platelet type) bainites in case of grade A is better than grade B.

After annealing treatment, the microstructure of both the grades consist of spheroidal graphite embedded in a ferrite matrix but the number of nodules is higher in the copper enriched grade. So, both the structures show high ductility but lower values of hardness and strength. After air cooling or normalizing, the microstructures in both the cases show a typical “bull’s eye” structure in which most of the graphite nodules are surrounded by a ferritic envelope. Both the graphite nodules and ferritic envelopes are embedded in a pearlitic matrix. When quenching and tempering is done, the microstructure consists of a martensite matrix with graphite nodules. After tempering at higher temperatures, the matrix phase changes to tempered martensite, thus relieving the internal stresses and increasing the strength and ductility, compromising with hardness.[17,20]

After austempering treatment, the entire matrix changes to plate-like ausferrite and/or bainitc ferrite and high carbon austenite in both the cases. Graphite nodules are embedded in the matrix, as shown in figure4.2.1 from (k) to (r).At lower austempering time, very fine needle-type or acicular bainitic ferrite are observed with small amount of retained austenite and some martensite, which increases the strength. But as the austempering time increases this fine structure with no martensite appears and increases the strength and decreases the ductility and hardness due to disappearance of martensite and with increase in bainitic ferrite .This relates the

microstructure with the mechanical properties. So there is an optimum value of time and temperature of treatment to obtain a good combination of strength and properties.[28]

4. 2.2 Fractrography:

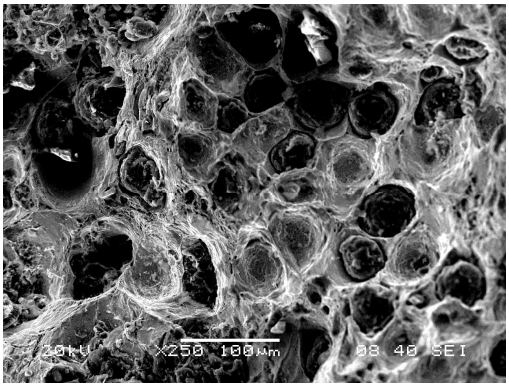

(a)As-cast (GdA)

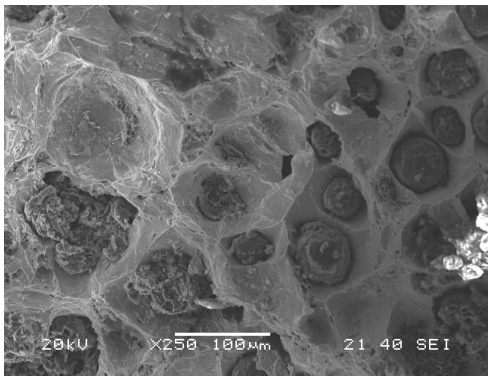

(b) As-cast (Gd B)

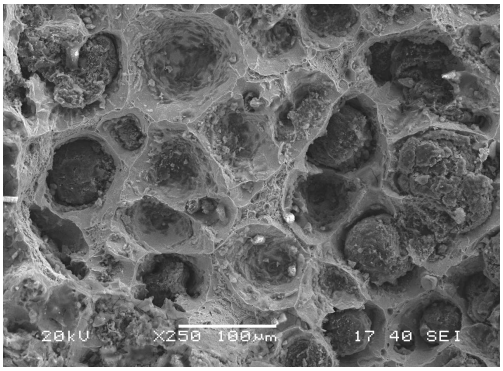

(c)Annealed (Gd A)

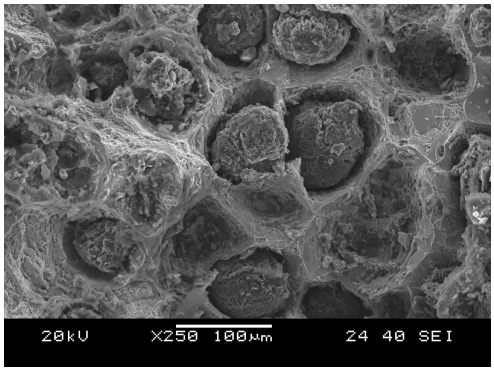

(d) Annealed (GdB)

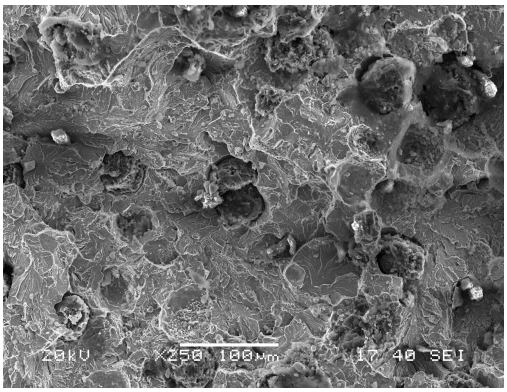

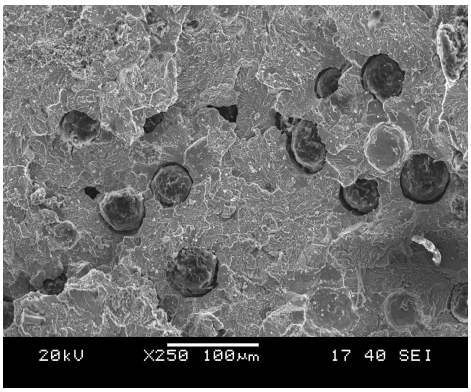

(e) Normalized (Gd A)

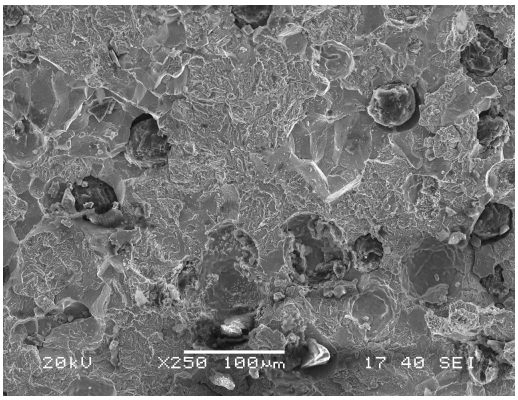

(f) Normalized (Gd B)

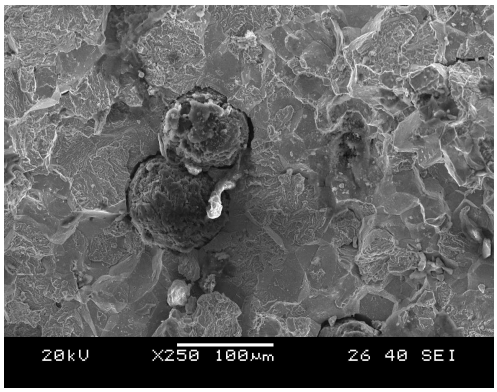

(g)Tempered2 (Gd A)

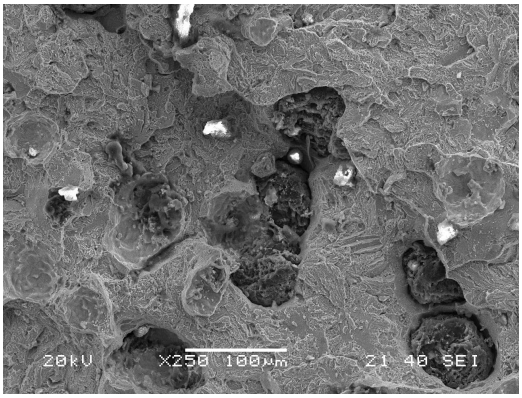

(h) Tempered2 (Gd B)

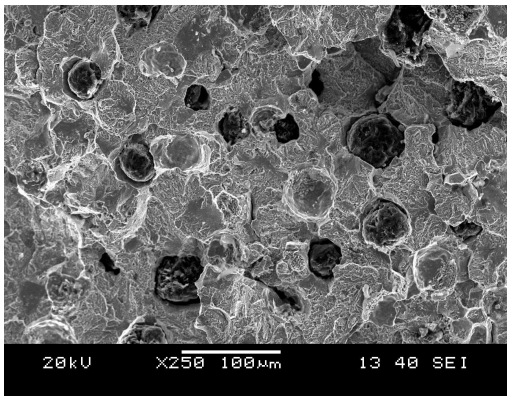

(i)Tempered 4(Gd A)

(j) Tempered 4 (Gd B)

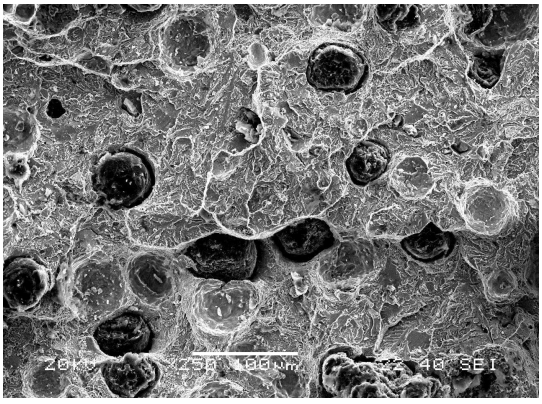

(k) Tempered6 (Gd A)

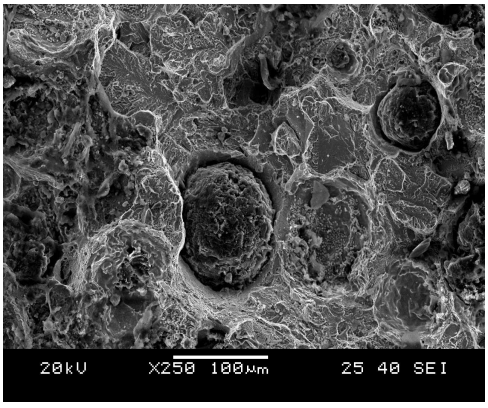

(l) Tempered 6(Gd B)

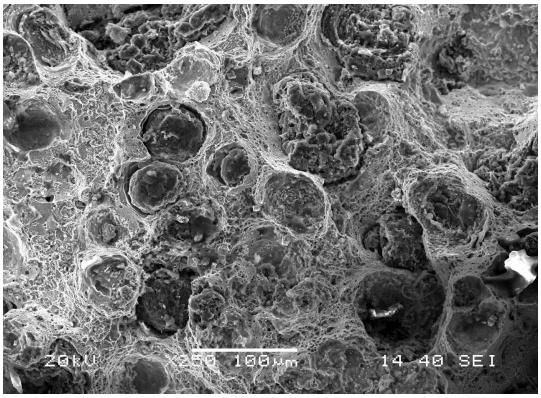

(m)Austempered0.5 (Gd A)

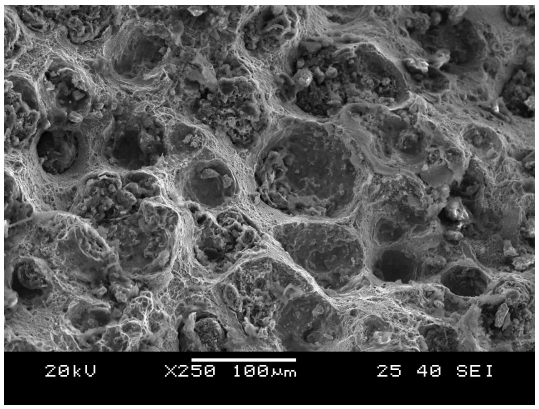

(n)Austempered 0.5(Gd B)

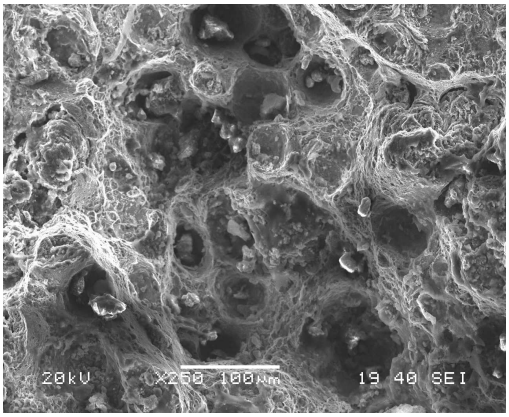

(o) Austempered 1(Gd A)

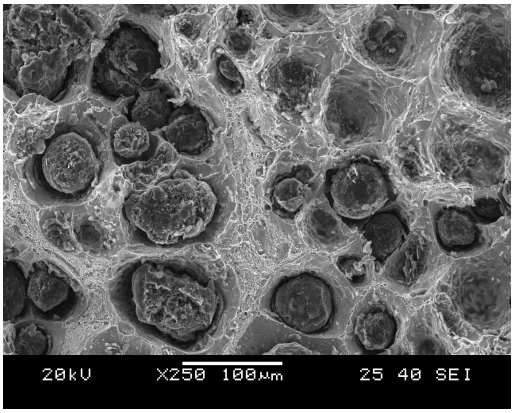

(p) Austempered 1(Gd B)

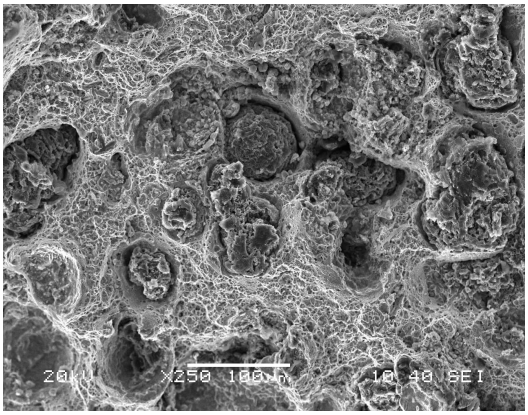

(q) Austempered 1.5 (Gd A)

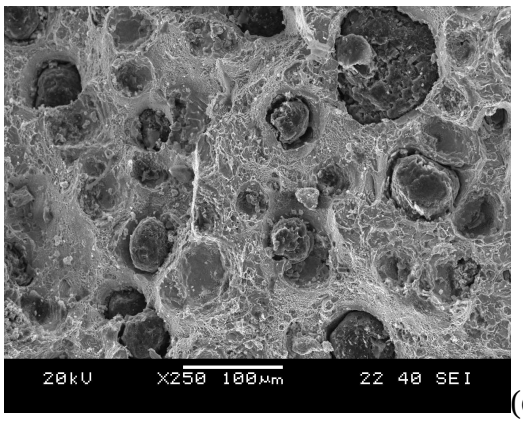

(q)

(r) Austempered 1.5 (Gd B)

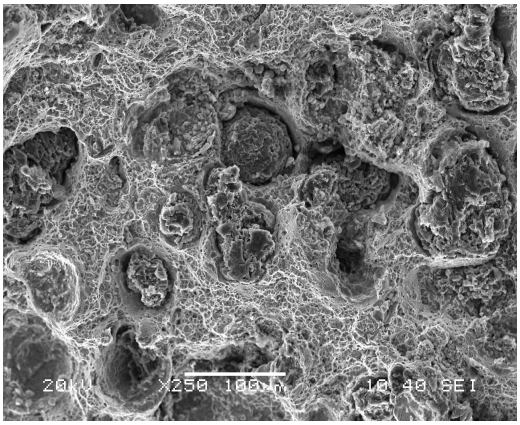

(s) Austempered 2(Gd A)

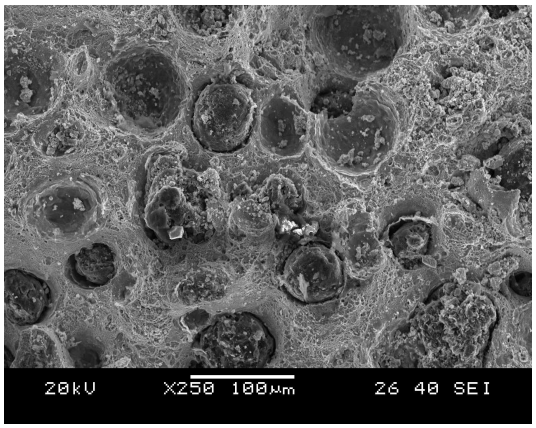

(t) Austempered 2(Gd B)

Fig 4.2.2: Fracture Surface of untreated and treated samples after tensile testing.

*Gd A and Gd B: Samples with Cu and Without Cu

*Tempered 2, 4, 6: tempered at 200, 400 and 600°C.

*Austempered 0.5, 1, 1.5, 2: Austempered for 30, 60, 90, 120 minutes.

The morphology of the fracture specimens are analyzed by Scanning Electron Microscopy (SEM). Figure 4.2.2 shows the fracture surface of the different samples. As cast ductile iron shows a fully dimpled fracture. The fracture pattern in annealed samples are same as in as cast ductile iron with greater numbers of dimples as shown in fig4.2.2(c)and (d) , while the fracture in normalized samples show a brittle fracture with river patterns in the vicinity of pearlitic areas as shown in fig4.2.2(e) and (f), for both the grades. So, the fracture surfaces confirms with the high ductility in annealed samples and low ductility in normalized samples. The fracture pattern of tempered samples at low temperatures show a mixed mode of fracture because of the untransformed martensite presents at that temperature, but as the tempering temperature increases the major fracture pattern is ductile in nature. So, this conforms to the increase in ductility i.e. the elongation percentage. There is decrease in strength and hardness when tempering temperature is increased from 200°C to 400°C. But, the strength and hardness values remain constant with further increase in tempering temperature to 600°C. This is due to the occurrence of strain-hardening phenomena. [17]

In case of austempering treatment, at lower treatment times, the fracture pattern (in both the grades) shows a mixed mode of fracture (ductile and brittle), because of the presence of retained austenite and some amount of martensite. But as austempering time is increased, the fracture bears a dimple type appearance because of the disappearance of martensite phase. But, if time is further increased, brittle fracture dominates. [28, 30]

4.3 X-Ray Diffraction:

The X-Ray diffractgrams are taken on some selected samples in both as received condition and treated condition to study the phase changes taking place during various treatment; are presented in Figure 4.3(a) to (f).

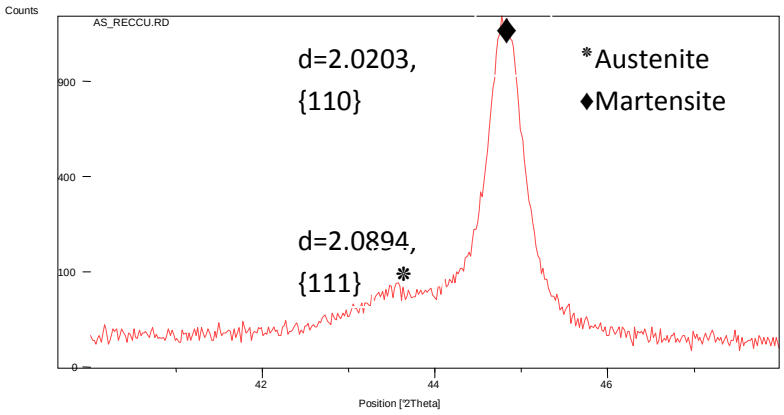

(a)

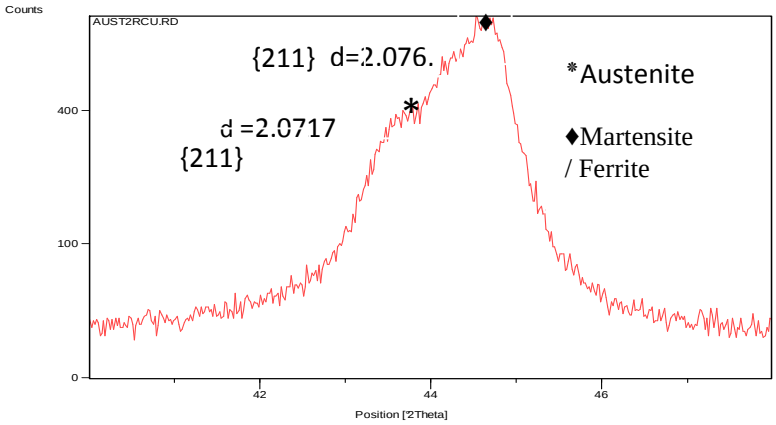

(b)

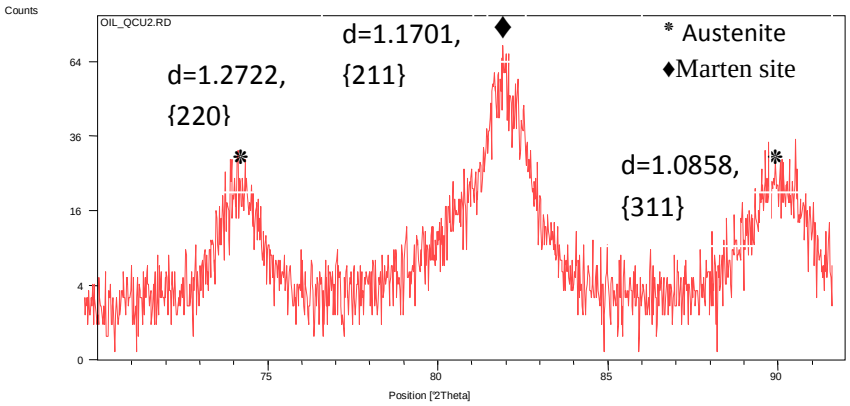
Counts
OIL_QCU2.RD
d=1.1701,
{211}
* Austenite
♦Marten site
d=1.2722,
{220}
d=1.0858,
{311}
64
36
16
4
0
75
80
85
90
Position [°2Theta]

(c)

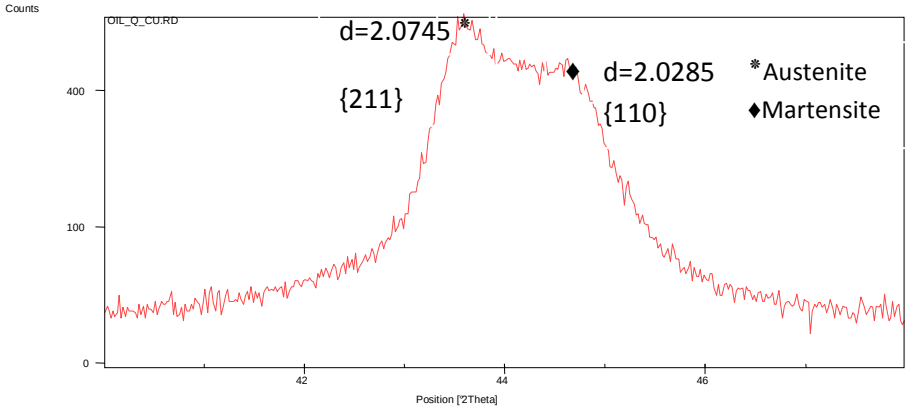
Counts
OIL_Q_CU.RD
d=2.0745
{211}
d=2.0285
{110}
*Austenite
♦Martensite
400
100
0
42
44
46
Position [°2Theta]

(d)

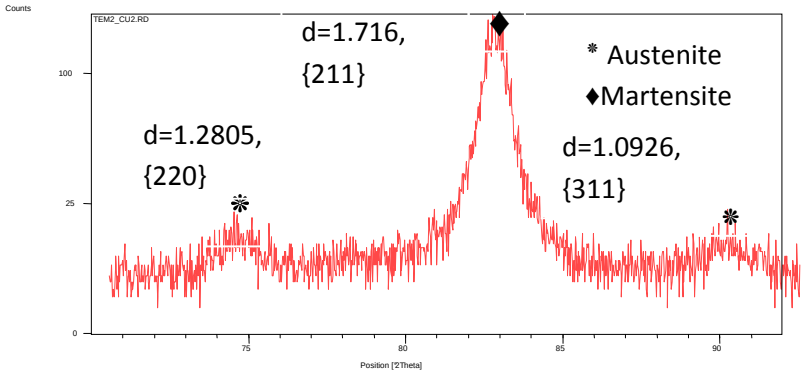
Counts
TEM2_CU2.RD
d=1.716,
{211}
* Austenite
♦Martensite
d=1.2805,
{220}
d=1.0926,
{311}
100
25
0
75
80
85
90
Position [°2Theta]

(e)

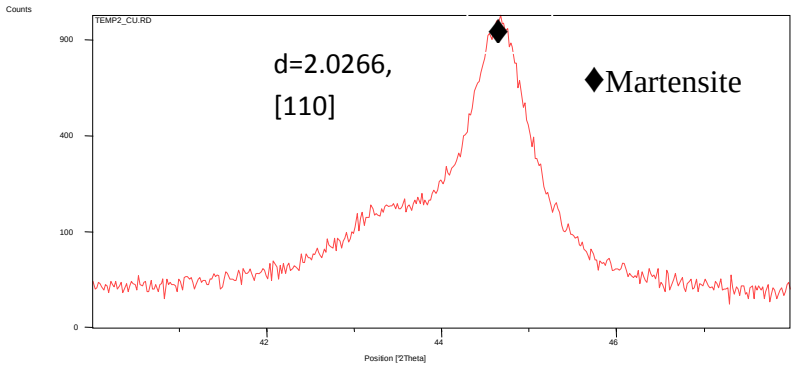

(f)

Fig 4.3: Diffraction patterns of untreated and some treated samples.

Comparing the as received sample and austempered samples given in figure 4.3(a) and (b), it is found that in as received sample there is a little amount of austenite phase (may be retained austenite) and pearlite phase content is much higher i.e. > 80%. While, in austempered samples for (2 hours) the amount of retained austenite is little higher than as received samples. The amount of retained austenite increases with time and this may be explained taking into account the bainitic transformation is not completed by that time.[25,29]

Comparing the XRD of quenched and tempered samples shown in figure 4.3(c) to (f).It is found that in tempered samples (at 200°C), affects the martensite/ tempered marensite phase and reduction of austenite percentage, as revealed from the variation of intensity of the peaks of both the samples.[17]

CHAPTER5

Conclusion

Conclusion:

The correlation between the microstructures and mechanical properties of Ductile Iron were studied along with their fracture surfaces for two different heat treatment processes- Quenching and Tempering; and Austempering. We also studied the effect of Copper on the microstructures, mechanical properties and fracture surfaces after heat treating.

For **Quenching and Tempering heat treatment cycle,** we observed the following:

1. As the tempering temperature increases, ductility of the samples also increased but compromising with hardness and strength.
2. The strength and hardness values were more for the sample with copper while ductility was found to be more for the sample without copper.
3. The fracture surfaces showed a mixed mode of fracture for both the grades of samples. But, the percentage of dimple fracture was found to increase with tempering temperature.
4. The microstructure in as cast condition shows the pearlitic matrix with graphite nodules in both grades of samples, while after qunehing and tempering the matrix converted into the martensite and tempered martensite. Thus, the strength and elongation was increased in tempered samples, but hardness decreases.

For **Austempering heat treatment cycle,** we observed the following:

1. As the holding time for austempering increases, the tensile strength initially increases and then decreases. Contrary to it, % elongation first decreases and then increases with time. The hardness values normally decreases with austempering time.

2. The strength and hardness values for the sample with copper are more while ductility was found to be more for the sample without copper.

3. The fracture surfaces showed a mixed mode of fracture for shorter austempering time. The percentage of dimple fracture then increased with time. For longer austempering time, percentage of cleavage fracture was found to be more.

4. The microstructure was ausferrite or bainitic ferrite and retained austenite with graphite nodules embedded in it for all periods of time. But, the morphology of bainite was changed from needles to plate like structure as the austempering time increases. So, the strength and hardness decreases with time and ductility.

FUTURE SCOPE

Engineering applications of ductile iron in as cast and different heat treated conditions are growing day by day. Austempered Ductile Iron's application has increased tremendously in many industrial areas. Austempered Ductile Iron is increasingly the material of choice of designers and engineers because of their cost effective performance. It has started to replace steel in some structural applications. It has also found it's tremendous applications in automobile sector which includes crankshafts, disc-brake calipers, axle housings, etc. It is also used to manufacture spun pipes, pump bodies, rock drillers, etc. For all these applications, we need to take into consideration many other mechanical properties like, wear and erosion resistance, impact resistance, fracture toughness, creep resistance, noise reduction and energy saving properties, etc. So in future, we can measure the above mentioned mechanical properties to optimally select a material for its specific application.

References

1. 1. Siefer W. and Orths K., Transection AFS, volume 78, 1970, Pages 382-387.
2. R.D. Forrest, “Some factors affecting the mechanical properties ductile iron”, January1989, Pages 23-37.
3. Karsay, “S.I. ductile Iron I”: Production (revised in 1976) the state of the art, 1976, Sorel, Canda, Quebec Iron and Titanium, 1977.
4. R.D.Forrest, J.D Mullins, “Achieving and maintaining optimum ductile iron metal quality”, Foundry, An Indian Journal for Progressive Metal-Casting, volume xv, no.4, July-August2003, Pages51-58.
5. Karsay, “Production of S.G. Irons”.
6. A guide to mechanical properties of ductile iron, Mid- Atlantic Casting service.
7. Metal Handbook, Volume 9, chapter 6, Pages 70-90.
8. S.P. Oudhira, “Quality demand an S.G. Iron Casting”, Foundry, An Indian Journal for Progressive Metal-Casting, volume X No.4, July-August, 1998, Pages 5-10.
9. Prof. S.N. Iyengar, “A short history of the birth and development of S.G. Iron in the Initial years”, Foundry, An Indian Journal for Progressive Metal-Casting, Volume.x, No.6, Nov-Dec 1998, Pages 9-10.
10. BCIRA Broadsheet 212: Factors influencing the ductile or brittle behavior of nodular irons.
11. Barton, R. “the selection of carbon and silicon contents in the production of as-cast and heat treated SG iron. Paper presented at: Proceeding of the Third International Conference of I.icensees for the Converter Process”, Schaffhausen, Switzerland, 7-10 October 1979, Paper -1
12. Unpublished work at BCIRA.
13. Davis J.R., ASM Specialty Handbook: Cast Irons, ASM International, 1996, pages 437.
14. Hughes I.C.H., Austempered ductile iron: their properties and significance, Materials & Design Vol. 6, July 1985.
15. Yan Mi. Scripta Metallurgica and Material, Volume32, 1995, Pages13-14.
16. Study of the engineering properties of ductile, Technical report of ductile iron.

17. Ali.Rashidi M. and Moshrefi-Torbati M.; Effect of tempering conditions on the mechanical properties of ductile cast iron with dual matrix structure (DMS). Material Letters, Vol. 45,Issue 3-4,September 2000,page 203-207.
18. .Choi J.O, .Kim J.Y, Choi,C.O; Effect Of rare earth elements on microstructure formation and mechanical properties of thin walled ductile iron casting. Material Science and Engineering A, volume 383, Issue 2, 15 October 2004, pages 323-333.
19. Fatahalla. N., Bahi. S.; Metallurgical parameters, mechanical properties and machinability of ductile cast iron, Journal of Materials Science 31 (1996) 5765 5772.
20. Morrogh H., Influence of some residual elements & their neutralization in Magnesium treated noduler cast iron. Source book of ductile iron.
21. .Chang L.C, Hsui I.C, Chen L.H. and Lui T.S ; A study on particle erosion behavior of ductile irons, Scripta Materialla, Vol 56, Issue 7, April 2005, page 609-613.
22. Olivera. E., Jovanovic Milan.et.al; The austempering study of alloyed ductile iron, Materials and Design, Volume 27, 2006, Pages 617–622.
23. Putatunda Susil K., Kesani Sharath et. al.; Development of austenite free ADI (austempered ductile cast iron), Materials Science and Engineering A, July 2006, Pages 112–122.
24. Shelton P.W.,Bonner, A.A.;The effect of copper additions to the mechanical properties of austempered ductile iron (ADI), Journal of Materials Processing Technology, June 2005, pages 269-274.
25. Kocatepe. Kadir, Cerah Melika, Erdogan Mehmet; The tensile fracture behaviour of intercritically annealed and quenched + tempered ferritic ductile iron with dual matrix structure; Journal of Materials and Design, July 2005, Pages 172-181.
26. Hafiz M.; Mechanical properties of SG-iron with different matrix structure; journal of Material Science, Volume 36, 2001, Pages 1293-1300.
27. Eric O., Rajnovic Dragan, Zec S lavica et. al.; Microstructure and fracture of alloyed austempered ductile iron; Materials Characterization, Volume 57, January 2006, Pages 211-217.

28. Kim Yoon-Jun, Shin Hochoel; Investigation into mechanical properties of austempered ductile cast iron(ADI) in accordance with austempering temperature; Materials Letters, Volume 62, May 2006, Pages 357-360.
29. Toktaş Gulcan, Tayanç Mustafa et. al.; Effect of matrix structure on the impact properties of an alloyed ductile iron; Materials Characterization, Volume 57, Febraury 2006, Pages 290-299.
30. Kumari Ritha U., Rao Prasad P.;Study of wear behaviour of austempered ductile iron; Journal of Material Science, Volume 44, January 2009, Pages 1082-1093.
31. Cavallini M., Bartolomeo O. Di et.al.; Fatigue crack propagation damaging micromechanism in ductile cast irons, Engineering Fracture Mechanics, Volume 75, February 2007, Pages 694-704.
32. Stokes B., Gao N., Reed P.A.S.; Effects of graphite nodules on crack growth behavior of austempered ductile iron; Materials Science and Engineering A; September 2006, Pages 374-385.
33. Kutsov A., Taran Y. et.al.; Formation of bainite in ductile iron; Materials Science and Engineering A, 1999, Pages 480-484.
34. Ayman Elsayed H., Megahed M.M. et. al.; Fracture toughness characterization of austempered ductile iron produced using both conventional and two-step austempering processes; Materials and Design, Volume 30, September 2008, Pages 1866-1877.
35. Haseeb A.S.M.A., Islam Aminul et.al.; Tribological behaviour of quenched and tempered, and austempered ductile iron at the same hardness level; Journal of Wear, April 2000, Pages 15-19.
36. Jaun Manuel Velez, Tanaka V.K; Metallurgical & Material Transaction A, Volume 29, December 1999, pages 2925-2934.
37. Shaker M.A.; a note on the effect of nodulerization characteristics on the workability of quenched- hardened and tempered cast iron. Journal of Material processing technology, Volume 32, Issue 3, August 1992, pages 545-552.
38. D'Amato C, Verdu C, Kleber X. et. al.; Characterization of Austempered Ductile Iron through Barkhausen Noise Measurements; Journal of Nondestructive Evaluation, Vol. 22, No. 4, December 2003.

39. Eric O., Sidjanin L., Miskovic Z. et. al.; Microstructure and toughness of Cu-Ni -Mo austempered ductile iron; Materials Letters, Volume 58, June 2004, Pages 2707– 2711.
40. Kiani-Rashid A.R., Influence of austenitising conditions and aluminum content on microstructure and properties of ductile irons; Journal of Alloys and Compounds, Volume xxx, February 2008.
41. Weesan Magnus, Ingvar L.; studied the growth of ferrite in noduler cast iron by thermal analysis of cooling in plate casting; Metallurgical and material Transection A, Volume 29 A, December 1998, Pages 3061-3072.
42. Heydarzadeh M., Ahmadabadi Nilli M.; The role of austempering parameter on the structure and mechanical properties of heavy section ADI, Journal of Material processing Technology, Volume 153-154, November 2004, Pages 203-208.
43. Zhao W. and Guixin W.; Metallurgical and Material Transaction A, Volume 28 a, July 1997,Pages 1121-1132.
44. Nilson Fedrick Karl and Blagovea D.; An experimental and numerical analysis to correlate the variation in ductiltity and defeacts of microstructure in ductile cast iron components; Engineering Fracture Mechanics, Volume 73, Issue 9, June 2005, Page 1133-1147.
45. Monchoux J.P. and Vedru C.; Effect of Ferritization Heat Treatment on the fracture toughness of ferritic spheroidal graphite cast iron.
46. Zhu J.H. and Liaw P.K.; Metallurgical and Material Transection B, Volume 29A, November 1998, Page 2885-2862.
47. Shiao F.T. and Liu T.S.; Metallurgical and Material Transaction B, Volume 30A, July 1999, Pages 1775- 1785.
48. Kong Zhou, Yehua Jiang, Dchong Lu, Rongfeng Zhou and zhenhua L; Journal of Wear, Volume 250, July 2000, Pages 280-288.
49. Eric O, Sidjanin L, Zec S, Jovanovic MT. Mater Letters,2004, Volume 58, Pages 2707–11.
50. Introduction to Physical Metallurgy; Sidney H. Avenar.
51. Mechanical Metallurgy; G.E.Dieter New York: McGraw-Hill Co.;

52. ASM, “Metals Handbook- Metallography and Microstructures, Volume 9, 9th ed. (American Society of Metals).
53. G. Krauss, Principles of Heat Treatment of Steel, ASM, 1980.
54. Heat treating of cast iron, Source Book on Ductile Iron, ASM, 1977, Pages 185–202.
55. ASM, “Metals Handbook,” Vol. 15, 9th edition (American Society of Metals, Metal Park, Ohio, USA,) 1992.
56. Hafiz M. Tensile properties and fracture of ferritic SG-iron having different-shell structure. Z Metallkd Volume 11, 2001, Volume 1258–61.
57. Tewari S.N.; Cast Iron Technology, Volume 1.

.